

Referee #1

Major comments

1. All three datasets are of dubious accuracy in representing interannual variability. The annual totals computed from eddy covariance sum much larger fluxes of opposing signs with likely systematic biases, especially in nighttime. The empirical upscaling was found to have relatively weak performance in representing interannual variability in a synthetic data experiment (without even accounting for any measurement or representativeness error in the training set) reported by Jung et al. (2009), for which the absence of soil moisture as a predictor is given by them as one reason. The inversion estimate, as the authors point out, is dominated at sub-continental scales by the (reasonable) prior assumption that variability scales with modeled NPP, and it probably contains little actual information from the CO₂ time series at those scales. Could it make sense to run the inversion with a more 'flat' prior, or a prior based on the MPI-MTE IAV, to get different IAV estimates?

We agree with the reviewer that all the datasets used in the present analyses present weaknesses and lack of accuracy in representing the inter-annual variability. On the other hand, this is what is currently available in terms of global-scale data of CO₂ land fluxes derived from inversions of atmospheric measurements or from the upscaling of surface flux observations. Following the reviewer suggestion, the limits of each product were better discussed in the Materials and Methods section and strengths and weaknesses were taken into account when evaluating results.

Concerning the prior used for the Jena Inversion, it has indeed a seasonal pattern, however this is constant from one year to another, hence there is no influence of the prior on the IAV. The prior can only influence the fine-scale spatial pattern of IAV, since in the optimization the fluxes scale in space with the average prior flux. On the contrary the temporal IAV derives fully from the atmospheric signal. Therefore in terms of IAV running the inversion with a "flat" prior will not make any difference compared to the current analysis.

On the contrary, using an MPI-MTE based prior for the Jena Inversion product would contaminate the IAV estimation, mostly because MPI-MTE varies in time, hence MPI-MTE IAV would influence the IAV derived from the Jena Inversion with the result that the two products wouldn't be independent any more.

2. Figure 4 shows the dependence of median(?) IAV on resolution for the two gridded products. I wonder if something like this could be done with the available Fluxnet stations as well, for example with the help of a variogram (mean covariance of de-seasonalized NEE time series as a function of inter-station distance). This could help in deciding whether the lower IAV in the gridded products compared to Fluxnet is only because of the difference in spatial scale or is more intrinsic.

We thank the reviewer for the interesting suggestion. Following this advice we added new data-series to Fig 4 to explore the dependence of IAV on the spatial averaging of the Fluxnet dataset, following the scheme used for the gridded product. The new series represents the IAV

calculated from the Fluxnet database as a function of the area of aggregation of the sites, starting from single sites and then proceeding with averaging time series for groups of sites located within an increasing distance. This procedure applied to flux sites mimics a decreasing resolution as done for the gridded products.

3. I didn't see any analysis of to what extent the IAV between the three products is actually in phase (i.e. the correlation of the deseasonalized NEE time series between the datasets). It would probably be relevant to show this.

We have taken this point in consideration together with point #1 raised by reviewer #3 and performed an analysis on the temporal correlation between the global averages of the two global products and of the Global Carbon Project estimates. See new Figure 11 and related text.

4. Also, forest inventories and crop yield statistics provide more reliable direct measurements of (at least above-ground) NPP and its IAV in many countries, potentially with rather good spatial coverage. Would there be any way to compare these to the IAV in the data sets reported here?

Following the suggestion of the reviewer we considered other possible data streams for the analysis but ultimately concluded that neither forest inventory nor yield statistics are appropriate for the present analysis. In fact, forest inventories are typically performed every 10-15 years, therefore they report NPP as a time average and for this reason they cannot be used in an inter-annual variability analysis. On the other hand crop yields are not necessarily correlated to primary productivity, as they may be affected by events that do not affect GPP like for example a storm or frost at the end of the growing season that can fully compromise the yield but do not substantially change GPP.

Minor points

1. The element "carbon" is not capitalized (title and line 287).
The typo was corrected.
2. Line 25: no comma before "that"
Comma was cancelled
3. Figure 1c: It would be good to show the station network on the map.
Following the reviewer suggestion the station network was plotted in Figure 1c
4. "Anomalies" sounds strange as a description of the IAV residuals from linear trend shown in Figure 5 and discussed in the text. Perhaps there is a better term.
As suggested by the reviewer we used the term residuals.
5. The Jung et al. (2009) citation should be to the final paper, not the discussion paper.
The citation was replaced with that of the final paper.
6. Formatting in the bibliography needs to be fixed, e.g. for Morgenstern et al. (2004) and others.
Bibliography was checked and fixed.

Referee #2

General comments

1. There are some weaknesses. Some areas of the text, and a critical point or two in the methods, are unclear. Neither the MPI-MTE nor the inversion products seem ideal for this kind of IAV analysis, although I recognize that this is all there is to work with; still, the authors should address this.

As stated by the reviewers the dataset used in the analysis are those available nowadays for the land CO₂ fluxes, namely i) site observations based on eddy covariance, ii) statistically upscaled products derived from site level measurements as MPI-MTE, or iii) inversion modeling products. We are aware of the weaknesses of the products used in this analysis and we better discussed them together with their pros both in product descriptions and in the result discussion. Refer also to Referee #1 comment 1.

2. In addition, the conclusion should be re-done or removed; on a related note, the strengths and weaknesses of these NEE data products might be better, and more succinctly, summarized based on the analyses performed.

Following the suggestions of reviewer #2 and #3 we wrote two new paragraphs at the end of the Result and Discussion section as Conclusions.

Specific comments

1. Lines 118-120: not as clear as it should be. Interannual variability computed with a 12-month window? How is this possible, as that's only 1 year?

Analysis of IAV was based on the entire time series. Annual values were calculated not only for the "solar" years which were available in the dataset, but additional "years" were generated using a 12-month moving window which was shifted one month a time, following the methodology proposed by Luysaert et al. (2007).

2. L. 171-172: move to figure caption, or methods

The sentence was moved to Materials and Methods section 2.2

3. L. 197: "area of"

The typo was corrected

4. L. 241-243: unclear

We better clarified the concept in the revised text on the basis of what follows.

The impact of climate drivers on IAV is based on a spatial analysis and not a temporal one. Spatial analyses of IAV in the inversion product are critical because at fine scale the spatial variability of the fluxes is mainly controlled by priors. In fact, the optimization algorithm of the inversion spatially allocates the fluxes proportionally to the prior; hence grid cells with higher productivity will change more if compared to cells with lower prior value (i.e. IAV at fine scale is proportional to the prior). For this reason we did not perform the spatial analysis on the inversion. On the contrary, prior does not affect the temporal analysis of IAV performed on the inversion product throughout the paper.

5. L. 250-: separating paragraphs, or indenting their first lines, would make this easier to read
Following the reviewer suggestion paragraph first lines were indented.
6. L. 286-: these aren't conclusions, just a recapitulation of results; remove
As stated above we reformulated the conclusions in the new version of the manuscript.
7. Figure 2: Rain (in axis title) or Precipitation (in caption)?
Axis title was modified in order to be consistent with the figure caption

Referee #3

General comments

1. I feel like the paper is missing the bigger take home message I was looking for, to the globally (or Fluxnet) integrated anomalies in NEE match up with 1) each other and 2) anomalies in the land C sink the global carbon project (Le Quéré et al. 2014; these data are available in a downloadable spreadsheet at <http://www.globalcarbonproject.org/carbonbudget>)

Even though the focus of the paper is on the pattern of IAV, we agree with the reviewer on the usefulness of a global inter-comparison of anomalies between products and with the GCP. In the new version of the manuscript we therefore provided such a comparison, bearing in mind that GCP land fluxes are estimated as residual term from the atmospheric CO₂ budget and are therefore not completely independent from the inversion product.
2. Since the paper is ostensibly about inter-annual variability in the terrestrial C cycle (NEE) what aren't all data products detrended first (these are weak responses anyway caused by different assumptions made with each approach)? Then the authors would be better able to address the IAV (or anomalies) which seem to be the focus of the paper.

IAV is generally defined as the temporal variability of the annual flux as generated by trend and residuals (Yuan et al. 2009), for this reason in the manuscript we analyzed both components and quantified the relative magnitude of the two (e.g. Fig 5 show that IAV is dominated by the anomalies). We made this clearer in the new version of the manuscript.
3. What climate or weather data are used in MTE or the Jena inversion. Presumably neither used CRU (temperature) and GPCC (precipitation), as the authors of this paper chose to do? Thus, are analyses of climate drivers on IAV of NEE actually really just comparisons of distinct climate reanalysis products? Also, why not use the CRU precipitation product for consistency with the temperature data being used?

MPI-MTE is based on the same climate drivers adopted in this analysis, namely CRU for temperature and GPCC for precipitation (Jung et al. 2011), while Jena-Inversion is not using any climate data in the flux calculation (with the exception of the wind field), being purely based on the atmospheric concentration measurements and an inversion transport model. GPCC precipitation was used instead of CRU for consistency with MPI-MTE, besides nowadays it is considered a better product as far as precipitation is concerned.
4. Much of the text in section 3 is heavy on the results with little discussion and interpretation of the key findings. Although some sections do communicate broader statements about the findings (e.g. lines 197-206), similar thoughtful development of ideas should be included throughout this section

Following the advice of referee 2 and 3 in the revised version we expanded the discussion of the results presented in each figure.

5. Why aren't correlations of IAV with site – level or global-scale climate drivers shown for Fluxnet or Jena inversion products?

The analysis of the global climate drivers of IAV was performed with the MPI-MTE because it is the only gridded product suitable for this purpose. The analysis has not been performed on the Jena Inversion products for the reasons explained in Reviewer #2 Specific Comments #4. Besides, a site level analysis is beyond the scope of the paper since it has already been addressed in other papers (Luyssaert et al. 2007; Yuan et al. 2009; Wu et al. 2012).

6. I'm unclear what value is communicated by the calculation of CUP and CRP and would suggest removing these analyses from the paper. The finding that temperate and boreal systems have a stronger seasonal cycle in their CO₂ drawdown seems obvious from atmospheric CO₂ growth curves. Instead, if the purpose of these analysis is to "identify the role of photosynthesis and respiration as sources of IAV_NEE" (line 67), then it seems much more straightforward to just look at the IAV (or anomalies) of GPP and TER from the Fluxnet and MTE products directly. Then they could be correlated with climate drivers too? For example, at high latitudes do GPP and TER show strong temperature sensitivities, with anomalies GPP outpacing TER in warm years? Conversely, are Tropical GPP anomalies largely temperature related too, whereas TER shows less inter annual variability & climate sensitivity?

Since MPI-MTE and Fluxnet come from the same data source, while the Jena Inversion is a completely independent product, we think that it can be of interest to see if IAV patterns are consistent between products. Since atmospheric inversion does not allow to separate GPP and TER, we used CUP and CRP as their proxies and we tested the validity of this assumption. Results of this analysis are shown in Fig 9, where we can infer that CUP and CRP are dominated by GPP and TER respectively. Although not being perfect GPP and TER proxies, NEE_{CUP} and NEE_{CRP} are highly correlated with them. We believe that the analysis of CUP and CRP brings additional information when performed on the inversion product. In particular at high latitudes where GPP/TER partitioning performed as CUP/CRP is particularly clear. Please refer also to point 13 of the Specific comments. In addition, the separation of the ecosystem CO₂ fluxes in these two terms is becoming increasingly common since it allows the description of a plant phenology based on carbon fluxes instead of greenness indexes.

Specific comments

1. I'm not used to seeing citations in the abstract. Is that the format for this journal?
[Citation was removed.](#)
2. I'm used to seeing ecosystem respiration referred to as ER, but maybe the authors are used to using different conventions?
[Both acronyms are used in the literature on the topic.](#)
3. Line 55 This single paragraph is a single sentence consisting of a very long list of NEE estimation approaches. Why not break this into a sentence about each approach and discuss strengths/weaknesses of each?

We take this point and discussed further the strengths and weaknesses of the different approaches in the Materials/Methods sections.

4. Line 67 organization of objectives i), ii), and iii) don't align with the organization of methods and sections 3.1, 3.2 and 3.3. Can the objective reflect the broader layout of the paper?

Objective order was reorganized in accordance with the other sections of the manuscript.

5. I'd suggest Line 73 are "LaThuile and 2015" two distinct references?

These are two subsequent releases of the Fluxnet dataset namely La Thuille and the 2015 release which are available at: <http://fluxnet.fluxdata.org/data/la-thuille-dataset/> <http://fluxnet.fluxdata.org/data/fluxnet2015-dataset/> We added the links to the manuscript.

6. It's not clear if or how data were re-gridded (e.g. [1] subtracting finer scale RETRO and GFED4 fire fluxes from the Jena inversion, or [2] for temperature and precipitation in Fig. 2)

Both fire and meteo data were regridded using the aggregate function of the R-package raster, a sentence explaining this was added to the manuscript.

7. More broadly, is subtracting for fire fluxes even necessary? Do the 14 observations extrapolated to this global product even 'see' the effect of forest fires? Don't the atmospheric inversion products the global carbon project implicitly see the effects of these fires? If so, why should they be subtracted out here?

Inversion based estimates of land CO₂ fluxes include the signal of forest fires while MPI-MTE and Fluxnet don't. To maintain consistency in the analysis and to allow a proper comparison between products we decided to exclude fire driven IAV from the Jena Inversion product. We made this clearer in the revised text.

8. Line 80. There are enough abbreviations in the text already. Are these needed too? Their use in lines 210-219 makes the text very hard to follow.

Since the acronyms were only used in Fig 6, following the reviewer suggestion, they were removed from the text and explained in Figure 6 caption.

9. Line 109 Air should not be capitalized.

The typo was corrected.

10. 'Jena inversion' or 'Jena Inversion' should be used consistently throughout the text.

The spelling of the product name was homogenized throughout the manuscript.

11. Were any lagged correlations explored to see if climate variability affected NEE in the subsequent season / year?

Despite potentially interesting, lagged correlations between drivers and IAV were beyond the scope of the paper. In the present paper only spatial patterns of the IAV dependence on climate drivers were analyzed.

12. Standard deviation and IAV are used interchangeably throughout the manuscript, but I think they mean the same thing? If so, just one term should be used for consistency. If they are different, it should be clarified in the text.

The reviewer is correct the two terms can be used interchangeably to identify inter-annual variability as stated in Section 2.2 L1-2.

13. Line 133 I have no idea what this means "the difference between the two determination coefficients was computed" or where this analysis is presented (Fig 9)? More broadly, I'm

unclear how / why the authors tried to infer something about GPP and TER from the inversion product.

We agree with the reviewer that the sentence was not clear. We therefore improved the description of the analysis based on what follows.

Results of this analysis are presented in Figure 10 and 11. NEE was linearly correlated with GPP and TER (for Fluxnet sites and MPI-MTE, for which GPP and TER are available) and with NEE_{CUP} (where CUP stands for Carbon Uptake Period), and NEE_{CRP} (where CRP stands for Carbon release period) for the Jena Inversion product (for which GPP and TER are not available, and CUP and CRP were used as their proxies) to detect which of the two processes drives the IAV of NEE. The difference between the R^2 of the two regressions calculated for each pixel was plotted on maps in Fig 10 and in the climate space in Fig 11. The goodness of the assumption of CUP and CRP as proxies of GPP and TER was tested with the analysis shown in Fig 9.

14. Line 171. Why was IAV normalized using GPP estimates and not NEE, the latter giving a real coefficient of variation (CV; grid cell standard deviation NEE / mean grid cell NEE). This should be clarified both in the text and caption. Also, shouldn't grid cell CV be calculated first, and then averaged over each climate bin?

IAV was not normalized with NEE because the latter fluctuates around zero and can lead to unreliably high values of CV and to both positive and negative values. Normalization using GPP (which is always positive and significantly larger than zero) offers a more robust metric of relative IAV.

We use the ratio of the means because it is a more robust metric since mean of ratios is more sensitive to outliers if compared to the ratio of the means, besides the latter gives more weight to points that bear more information.

We clarified these methodological details in the revised document.

15. Line 180 & Fig. 3 I am unclear what insight this figure provides to the manuscript and it's sparingly discussed in the text. It's used to justify the CV calculation in Fig. 3 (line 173), but as this is a standard statistical approach I'm not sure it's warranted? As such, should the display item just be removed?

Fig 3 shows that in two data-streams (Fluxnet sites and Jena inversion) IAV increases monotonically and almost linearly with the productivity of the site. On the contrary MPI-MTE shows a different pattern, with a clear maximum followed by a decline of IAV in high productive sites. We think that this is due to the prominent role that FaPAR has in the MTE approach. Canopy greenness is particularly stable in the tropical humid forests (that are the most productive one) generating this unusual pattern of low relative IAV. We discussed this aspect in further details in the revised version, since it is relevant to understand the general performance of the MTE model in the representation of the global IAV patterns.

16. Line 200. It seems like 'trends' in IAV should be driven mainly by environmental presses like atmospheric CO₂ concentrations or broad-scale / chronic N deposition inputs. By contrast, climate variability, land use change, and fires should be responsible for 'anomalies' the dataset. Given that the Jena inversion depends strongly on modeled NPP products it's not surprising that it shows stronger 'trends' (see suggestion to detrend data, above). Also, it would be interesting to see if fire fluxes were not backed out of the Jena inversion (again mentioned above) how the

magnitude and timing of anomalies from these two data products compared to anomalies in the atmospheric CO₂ growth rate. This also could provide a better opportunities for the authors to illustrate the differences between the data products that are currently in the discussion.

As previously stated (Ref #1, General comment #1; Ref #2, Specific comment #4), the temporal dynamic of the land fluxes in the Jena inversion is totally driven by the atmospheric signal and fully independent from the prior, since the latter in this inversion scheme is time invariant. We argue that in the MTE product the lower IAV due to "trend" is due to the poor or lacking representation of environmental drivers like CO₂ or N deposition in this data product. We made this clearer in the revised version.

17. Line 296 Carbon should be lowercase

It was corrected.

18. The conclusion is really just a summary of results already presented (and repeated from the abstract). I'd omit this text, or say something more broadly about what we can infer from the study.

Conclusions were reformulated in the new version of the manuscript as requested by the reviewers.

19. Fig. 6 & 8 I know abbreviations for each plant functional type are given in the text, but not using them in the caption or x-axis label bar make this figure hard to understand.

Following the reviewer suggestion we removed the acronyms from the text and we added their explanation to the figure caption.

20. Fig. 6 Aren't there enough observations to include error estimates (or box-wisker plots) for Fluxnet sites?

Following the suggestion of the reviewer standard errors were plotted for Fluxnet PFT IAV values.

21. Fig. 7 Caption and text should use the same (consistent) terminology here. I'm not really clear what is being compared here? How does one calculate a spatial correlation coefficient on two single values (e.g., correlation of IAV~ mean temperature)?

The correlation was calculated in a moving spatial window of more than 600 points, we retrieved a IAV value and a temperature/precipitation value for each pixel. This was better clarified in the revised text.

22. Fig 7 The use of red-blue color bar on the left plots to show +/- correlation is confusing when on the right panels red-blue shows zonal mean correlations with trends or anomalies?

We take this point and changed the colors in the barplot to avoid misinterpretation of the figure.

23. Fig 8 If this part of the analysis stays in the revised manuscript, I'd suggest the caption should be more descriptive (what are red and green bars).

Additional information was added to the figure caption to make the figure more readable.

24. Fig 9 I really don't understand what this figure is showing. The text & figure caption are not clear. More, the inset showing Western Europe seems strange. If this figure remains in the paper at all, would it make more sense to 1) omit the inset or 2) put it into supplementary material?

This figure was better explained in the new version of the manuscript based on what follows.

The aim of the figure is to highlight the role of GPP and TER (for MPI-MTE and Fluxnet) and of their proxy NEE_{CUP} and NEE_{CRP} (for Jena Inversion) in building up IAV_{NEE} . The determination coefficients were calculated for each pixel (for the gridded products) or site (for Fluxnet) fitting linear regressions of IAV_{NEE} vs either GPP (TER), or NEE_{CUP} (NEE_{CRP}). The difference in determination coefficients of GPP and TER linear regressions (the same holds for NEE_{CUP} and NEE_{CRP}) was used as a measure of which driver affects more IAV_{NEE} . Blue zones are GPP/CUP driven zones being the difference $R_{GPP}^2 - R_{TER}^2$ (or $R_{CUP}^2 - R_{CRP}^2$) positive while red zones are TER/CRP driven. See also Reviewer#3 answer #13. The inset was included in the graph because of the high site density of flux sites that characterizes Europe. Plotting an enlarged map allows in our opinion a better visualization of results.

25. Fig 10 I also cannot understand I'm unclear what the color bar signifies (DR^2)? Is this the difference between TER/GPP when $NEE < 0$ during uptake periods and GPP/TER when $NEE > 0$ for MTE? If so, what does this difference of ratios really tell us? I also still unclear how this is translated onto the Jena data?

Figure 10 summarizes results plotted on maps in Figure 9 in a temperature/precipitation space. Blue pixels are GPP/CUP driven climate classes, red pixels are TER/CRP driven climate classes.

BIBLIOGRAPHY

- Jung M, Reichstein M, Margolis H a., Cescatti A, Richardson AD, Arain MA, Arneth A, Bernhofer C, Bonal D, Chen J, Gianelle D, Gobron N, Kiely G, Kutsch W, Lasslop G, Law BE, Lindroth A, Merbold L, Montagnani L, Moors EJ, Papale D, Sottocornola M, Vaccari F, Williams C (2011) Global patterns of land-atmosphere fluxes of carbon dioxide, latent heat, and sensible heat derived from eddy covariance, satellite, and meteorological observations. *J Geophys Res* 116:G00J07. doi: 10.1029/2010JG001566
- Luyssaert S, Janssens I a., Sulkava M, Papale D, Dolman a. J, Reichstein M, Hollmén J, Martin JG, Suni T, Vesala T, Loustau D, Law BE, Moors EJ (2007) Photosynthesis drives anomalies in net carbon-exchange of pine forests at different latitudes. *Glob Chang Biol* 13:2110–2127. doi: 10.1111/j.1365-2486.2007.01432.x
- Wu J, van der Linden L, Lasslop G, Carvalhais N, Pilegaard K, Beier C, Ibrom A (2012) Effects of climate variability and functional changes on the interannual variation of the carbon balance in a temperate deciduous forest. *Biogeosciences* 9:13–28. doi: 10.5194/bg-9-13-2012
- Yuan W, Luo Y, Richardson AD, Oren R, Luyssaert S, Janssens I a., Ceulemans R, Zhou X, Grunwald T, Aubinet M, Bernhofer C, Baldocchi DD, Chen J, Dunn AL, Deforest JL, Dragoni D, Goldstein AH, Moors E, William Munger J, Monson RK, Suyker AE, Starr G, Scott RL, Tenhunen J, Verma SB, Vesala T, Wofsy SC (2009) Latitudinal patterns of magnitude and interannual variability in net ecosystem exchange regulated by biological and environmental variables. *Glob Chang Biol* 15:2905–2920. doi: 10.1111/j.1365-2486.2009.01870.x

Patterns and controls of inter-annual variability in the terrestrial ~~Carbon-carbon~~ budget

Barbara Marcolla¹, Christian Rödenbeck², Alessandro Cescatti³

¹Fondazione Edmund Mach, IASMA Research and Innovation Centre, Sustainable Agro-ecosystems and Bioresources Department, 38010 San Michele all'Adige, Trento, Italy

²Max Planck Institute for Biogeochemistry, 07745 Jena, Germany.

³European Commission, Joint Research Centre, Directorate for Sustainable Resources, I-21027 Ispra (VA), Italy

Correspondence to: Alessandro Cescatti (alessandro.cescatti@ec.europa.eu)

Abstract. The terrestrial carbon fluxes show the largest variability among the components of the global carbon cycle and drive most of the temporal variations in the growth rate of atmospheric CO₂ (~~Le Quéré 2014~~). Understanding the environmental controls and trends of the terrestrial carbon budget is therefore essential to predict the future trajectories of the CO₂ airborne fraction and atmospheric concentrations. In the present work, patterns and controls of the inter-annual variability (IAV) of carbon Net Ecosystem Exchange (NEE) have been analysed using three different data-streams: ecosystem level observations from the FLUXNET database (La Thuille and 2015 releases), the MPI-MTE bottom-up product resulting from the global up-scaling of site-level fluxes, and the Jena CarboScope Inversion, a top-down estimate of surface fluxes obtained from observed CO₂ concentrations and an atmospheric transport model. Consistencies and discrepancies in the temporal and spatial patterns and in the climatic and physiological controls of IAV were investigated between the three data sources. [Results show that](#) the global average of IAV at FLUXNET sites (~120 gC m⁻² y⁻¹), quantified as the standard deviation of annual NEE, ~~was~~ observed to peak in arid ecosystems and to be almost six times larger than the values calculated from the two global products (15 and 20 gC m⁻² y⁻¹ for MPI-MTE and Jena ~~inversion~~[Inversion](#), respectively). The two data-driven global products show that most of the temporal variability observed in the last three decades is due to yearly anomalies, whereas the temporal trends explain only about 15% of the variability in the MPI-MTE product and 20% in the Jena Inversion product. Both at site level and at global scale, the IAV of NEE is driven by the gross primary productivity and in particular by the cumulative carbon flux during the months when land acts as a sink. Altogether these results offer a broad view on the magnitude, spatial patterns and environmental drivers of IAV from a variety of data sources; that can be instrumental to improve our understanding of the terrestrial carbon budget and to validate the predictions of land surface models.

1 Introduction

Atmospheric CO₂ concentration has been constantly increasing since the Industrial Revolution, and has caused a corresponding rise of 0.85 °C in the global air temperature from 1880 to 2012 (IPCC, 2013). Since the 1960s, terrestrial ecosystems have acted as a considerable sink ~~offer~~ atmospheric CO₂, reabsorbing about one quarter of anthropogenic emissions (Friedlingstein et al., 2010; Le Quéré et al., 2014). The growth rate of atmospheric CO₂ concentration is characterized by a large inter-annual variability (IAV), which mostly results from the variability of the CO₂ net ecosystem exchange (NEE) on land (Bousquet et al., 2000; Le Quere et al., 2009; Yuan et al., 2009). Multisite synthesis confirms that a large inter-annual variability in NEE is a common feature at all flux sites around the world (Baldocchi, 2008; Baldocchi et al., 2001). The reason why the IAV is so large is that NEE results from the small imbalance between two larger fluxes: the photosynthetic uptake of CO₂ (Gross Primary Production, GPP) and the respiratory release of CO₂ (Total Ecosystem Respiration, TER). As a consequence, even minor variation in either of the two fluxes can cause large variations in their difference.

40 It has been long debated which of GPP or TER controls the spatial and temporal variability of NEE. Several studies have ascribed inter-annual variability in NEE to variability in either GPP (Ahlstrom et al., 2015; Janssens et al., 2001; Jung et al., 2011, 2017; Stoy et al., 2009; Urbanski et al., 2007) or TER (Morgenstern et al., 2004; Valentini et al., 2000) or both (Ma et al., 2007; Wohlfahrt et al., 2008b). GPP and TER show comparable ranges of IAV, typically larger in absolute terms than that observed for NEE due to the temporal correlation between the two gross fluxes (Richardson et al., 2007). Given that
45 photosynthesis and respiration may respond differently to environmental drivers (Luyssaert et al., 2007; Polley et al., 2008), the interpretation of climate impacts on the variability of NEE requires the understanding of the relation between the IAV of NEE and that of GPP and TER (Polley et al., 2010).

The environmental factors driving the IAV of NEE (IAV_{NEE}) include: climate, physiology, phenology, natural and anthropogenic disturbances (Marcolla et al., 2011; Richardson et al., 2007; Shao et al., 2015). Understanding the spatio-
50 temporal variability of NEE and its controlling mechanisms is essential to assess the vulnerability of the terrestrial carbon budget, to evaluate the land mitigation potentials and to quantify the ecosystem capacity to store carbon under future climatic conditions (Heimann and Reichstein, 2008). Besides, quantifying inter-annual variability in NEE is a prerequisite for detecting longer-term trends or step changes in flux magnitude in response to climatic or anthropogenic influences and identifying its drivers (Cox et al., 2000; Lombardozzi et al., 2014).

55 The temporal dynamic of NEE has been addressed in numerous studies, based on either “top-down” approaches, which primarily focuses on aircraft atmospheric budgets (Leuning et al., 2004), tower based boundary layer observations (Bakwin et al., 2004) and tracer transport inversion (Baker et al., 2006; Gurney et al., 2002; Rödenbeck et al., 2003), or on “bottom-up” methods that rely on data-driven gridded products derived from the up-scaling of flux data (Jung et al., 2011, 2017; Papale et al., 2015; Papale and Valentini, 2003) or process-based biogeochemical models that simulate regional carbon budgets (Desai et al., 2008, 2007; Mahadevan et al., 2008).

60 Despite the broad literature on the subject, very few examples of IAV analysis based on multiple data streams are available in the literature (Desai et al., 2010; Pacala, 2001; Poulter et al., 2014). In the present study patterns and controls of the inter-annual variability of NEE have been analysed using three different data streams: ecosystem level data from the FLUXNET database, the MPI-MTE bottom-up product resulting from the statistical up-scaling of in-situ flux data (le Maire et al., 2010) and the Jena CarboScope Inversion top-down product, which estimates land (and ocean) fluxes from atmospheric CO₂ concentration measurements and atmospheric transport modelling (Rödenbeck et al., 2003). In particular,
65 this analysis aims to: i) assess the magnitude and the spatial pattern of IAV of NEE (IAV_{NEE}), ii) ~~investigate the role of key climatic variables, like temperature and precipitation, in driving the spatial pattern of IAV~~ investigate the role of key climatic variables, like temperature and precipitation, in driving the spatial pattern of IAV identify the role of photosynthesis and respiration as sources of IAV_{NEE} and iii) ~~identify the role of photosynthesis and respiration as sources of IAV_{NEE}~~ identify the role of photosynthesis and respiration as sources of IAV_{NEE} . Finally,
70 ~~investigate the role of key climatic variables like temperature and precipitation in driving the spatial pattern of IAV~~. Finally, the consistencies and discrepancies among the different data products are analysed and critically evaluated.

2 Materials and Methods

2.1 Datasets

75 Data at ecosystem scale were retrieved from two releases of the FLUXNET dataset, namely LaThuile (<http://fluxnet.fluxdata.org/data/la-thuille-dataset/>) and 2015 (<http://fluxnet.fluxdata.org/data/fluxnet2015-dataset/>). These datasets contain half-hourly data of carbon dioxide, water vapour and energy fluxes that are harmonized, standardized and gap-filled. Time series of NEE and of the component fluxes GPP and TER, together with air temperature and precipitation, were used in the present analysis. Flux data have the advantage to represent direct observations of in-situ IAV, however at most sites the time series are still too short for a proper analysis of the temporal variability of NEE (Shao et al., 2015). For
80 this reason only sites with a minimum of five years of observations and an open data distribution policy were selected. A

subset of 89 sites satisfied the two criteria, among which 27 evergreen needle-leaf forests (~~ENF~~), 5 Evergreen Broadleaf Forests (~~EBF~~), 12 deciduous broad-leaf forests (~~DBF~~), 6 mixed forests (~~MF~~), 12 grasslands (~~GRA~~), 8 croplands (~~CRO~~), 6 sites counting closed and open shrublands (~~CSH, OSH~~), 7 wetlands (~~WET~~) and 6 sites counting savannas and woody savannas (~~SAV, WSA~~).

85 At global scale, two sources of gridded data were used: a "bottom-up" data product, namely the MPI-MTE product (Jung et al., 2009) and, as "top-down" product, the Jena CarboScope CO₂ Inversion (Rödenbeck et al., 2003). The MPI-MTE dataset is built with a machine learning technique (model tree ensemble, MTE) to upscale in space and time the flux observations from the global network of eddy covariance sites (FLUXNET) integrated with climate and remote sensing data for the time period 1982-2011 (Jung et al., 2009). ~~Effects of land management, land use change and CO₂ fertilization are not represented in this product.~~ Global maps for GPP and TER at 0.5° spatial resolution and monthly temporal resolution were used, while NEE fields were calculated as difference between the gross fluxes. This product has become a reference dataset to evaluate process-oriented land models and remote sensing estimates of primary productivity. Another weakness of the product is despite the uneven distribution of eddy covariance sites, with many sites in the temperate regions and very few sites in the tropics on which it is trained.

90 . It integrates a large amount of in-situ measurements, remote sensing and meteorological observations using a machine learning technique and has been proved to reproduce well spatial patterns and seasonal variability of fluxes (Jung et al., 2009). On the other hand the product has some shortcomings: for instance the effects of land management, land use change and CO₂ fertilization are not represented. The MPI-MTE has been recognized to show poor performances in predunderestimate eting the inter-annual variability of carbon fluxes which has been ascribed to the low signal to noise ratio which leads to a little emphasis given to it in the model tree training. These limits may be due to the missing representation of ~~Besides, some key predictors-determinants of IAV are missing like changes in soil and biomass pools, disturbances (e.g. fires), ecosystem age, management activities and land use history. Finally, the lag between external forcing and ecosystem response is not represented in the product~~ (Jung et al., 2011). ~~Another weakness of the product is the uneven distribution of eddy covariance sites, with many sites in the temperate regions and very few sites in the tropics.~~

105 To derive surface fluxes, the Jena CarboScope Inversion combines modelled atmospheric transport with high-precision measurements of atmospheric CO₂ concentrations. Atmospheric transport is simulated by a global three-dimensional transport model driven by meteorological data. For consistency with the MPI-MTE product, monthly averaged NEE land fluxes from the s81_v3.6 version of the product were used here, at a spatial resolution of 5° x 3.75°. The Jena Inversion is particularly suited for the analysis of temporal trends and variability since it is based on a temporally constant observation network (14 atmospheric stations for the version s81_v3.6). Weaknesses of the Jena Inversion product are linked i) to the sparse density and biased spatial distribution of the sampling network, whose geometry affects the flux estimates in a systematic way, ii) to data gaps, iii) to measurement errors since the calculation is based on CO₂ data only, while atmospheric carbon comes also from CO and VOC, and iv) finally to -potential systematic errors of the transport model that cannot be assessed.

115 As the inversion estimates the total land flux, ~~it includes CO₂ emissions from fires in addition to NEE,~~ being calculated as the difference between the total surface flux and prescribed anthropogenic emissions, it includes also CO₂ emissions from fires in addition to NEE. For improving the consistency ~~with the other of the~~ two datasets (MPI-MTE and FLUXNET) ~~which that do not account for fire emissions,~~ we therefore subtracted fire emissions from the inversion estimates using an harmonized combination of the products RETRO (Schultz et al., 2008) for the period 1982-1996 and GFED4 (Van Der Werf et al., 2010) for the period 1997-2013. RETRO is a global gridded data sets (at 0.5° spatial resolution) for anthropogenic and vegetation fire emissions of several trace gases, covering the period from 1960 to 2000 with monthly time resolution. GFED4 combines satellite information on fire activity and vegetation productivity to estimate gridded monthly fire emissions at a spatial resolution of 0.25 degrees since 1997. RETRO and GFED4 were harmonized using the overlapping

years (1997-2000) to calculate calibration coefficients as the ratio of GFED4 to RETRO for latitudinal bands of 30°. The RETRO time series was then multiplied by these coefficients and the resulting time series of fire emissions was finally subtracted from the land flux of the Jena Inversion. It is worth noting that the remaining flux from the inversion is the sum of land use change emissions and NEE while the MPI-MTE does not account for the land use change flux.

In order to analyse the role of climatic drivers on the inter-annual variability, global maps of temperature and precipitation were used. Gridded ~~Air~~-air temperatures were obtained from the Climatic Research Unit (CRU) at the University of East Anglia at monthly time scale and 0.5°x0.5° spatial resolution, based on an archive of monthly mean temperatures provided by more than 4000 weather stations (Jones et al., 2012). Precipitation fields were obtained from the GPCP product at 0.5° and monthly time step (Schneider et al., 2014). This product is based on a large dataset of monthly precipitation from more than 85,000 stations and is provided by NOAA/ESRL PSD (Boulder, Colorado, USA). The MODIS MCD12C1 land cover product (Friedl and Brodley, 1997) was used to classify the land pixels and to calculate statistics by plant functional type. MCD12C1 provides the dominant land cover types at a spatial resolution of 0.05° using a supervised classification algorithm that is calibrated using a database of land cover training sites. Product resolutions were harmonized using the aggregate function of the raster R-package.

2.2 IAV Analysis

The inter-annual variability of NEE was estimated as the standard deviation of annual NEE values, as generated by trend and residuals, w. and computed on time windows of 12 months shifted with a monthly time step (Luyssaert et al. 2007; Shao et al., 2015; Yuan et al., 2009) and calculated with the same methodology for the three data-streams used in the analysis. Average values of IAV for plant functional type (PFT) were determined using the PFT classification of FLUXNET sites and the MCD12C1 product (aggregated at the appropriate spatial resolution using the dominant PFT) for the MPI-MTE and Jena Inversion. Map pixels/gridcells were also classified according to mean annual temperature and precipitation, and the mean value of IAV_{NEE} and normalized IAV_{NEE} were calculated for each climate bin.

For the two gridded products, which provide a 30 year long time series (1982-2011), the IAV was partitioned in two components, namely the variance explained by the temporal trend and that due to annual anomalies (Ahlstrom et al., 2015). For this purpose a linear model was fitted on the time series at each pixel, and the determination coefficient of the regression was used to measure the fraction of variance explained by the trend, whereas its complement to one was the fraction of variance due to anomalies.

The spatial correlation between IAV and climatic drivers (air temperature and precipitation) was analysed at global scale for the MPI-MTE by calculating the spatial correlation coefficient between the temporal standard deviation (IAV amplitude) of NEE and the average annual temperature or precipitation in moving spatial windows of 15°x11.5° (which means 31x21 pixels for MPI-MTE). The latitudinal averages of these correlation coefficients were calculated for latitudinal bands of 30°. This analysis was not replicated For this reason we did not perform this analysis on the Jena Inversion product.

Spatial analyses of IAV in the inversion product are critical because at fine scale the spatial variability of the fluxes in this product is mainly controlled by the prior estimates. In fact, the optimization algorithm of the inversion spatially allocates the fluxes proportionally to the prior; hence grid cells with higher productivity will change more if compared to cells with a lower prior. For this reason we did not perform this analysis on the Jena Inversion product.

Finally, in order to identify which process between photosynthesis and respiration drives IAV_{NEE}, for FLUXNET and MPI-MTE linear regressions between NEE and GPP ~~or and NEE and~~ TER were fitted for each site/pixel and the difference between the ~~two~~ determination coefficients of the two linear regressions was computed. Since GPP and TER cannot be derived from inversion products, we performed a similar analysis using NEE of the Carbon Uptake Period (CUP, sum of negative monthly NEEs) and of the Carbon Release Period (CRP, sum of positive monthly NEE), as proxies of GPP and TER for all the three data streams. Also in this case NEE was linearly correlated regressed with NEE_{CUP} and NEE_{CRP} to

~~detect which of the two processes drives the variability of NEE. Finally, IAV_{NEE} and IAV controls were also analysed in a climatic space defined by mean annual temperature and precipitation. Finally, annual anomalies of the two global products used in the present analysis were compared with the estimates derived from the Global Carbon Project (GCP) (Le Quéré 2016) data. Annual anomalies of the three data sources were analysed.~~

Comment [AC1]: I. Le Quéré, C. et al. Global Carbon Budget 2016. *Earth Syst. Sci. Data* 8, 605–649 (2016).

3 Results and Discussion

3.1 IAV patterns

~~Figure 1 shows the~~ The spatial pattern of inter-annual variability for the three data sets ~~is resumed in Figure 1.~~ The IAV of NEE at individual Fluxnet sites ranges from 15 to 400 gC m⁻²y⁻¹ and shows an average of 130 gC m⁻²y⁻¹. On average the most northern sites show a lower temporal variability both in Europe and in North America (Fig. 1a). A global map of IAV_{NEE} is shown also for MPI-MTE (Fig. 1b) and Jena Inversion (Fig. 1c) at the original spatial resolutions of the two products. The observed range of IAV is similar for the two gridded products and substantially lower than that observed at site level, probably due to the spatial averaging of the land fluxes that dampens the temporal variability. The mean global value of IAV is in fact 15 and 20 gC m⁻² y⁻¹ for MPI-MTE and Jena Inversion, respectively, and hence about one sixth of the site level IAV. The two gridded products confirm the decreasing trend of IAV toward northern latitudes observed at flux sites. A general decrease of IAV_{NEE} at higher latitude for both ENF and DBF was also observed by Yuan et al. (2009) although for none of the two PFTs these trends were significant.

In terms of IAV, the two global products show a reasonable qualitative correspondence for North America and Eurasia, whereas they disagree for South America, with MPI-MTE showing a minimum of IAV in the humid Tropics, where the inversion product shows ~~on the contrary a high large~~ variability. MPI-MTE in particular shows maximum values along the Eastern coast of South America while the Jena Inversion shows an almost opposite pattern. A similar behaviour is observed also in Africa, where the top-down product shows a maximum in central Africa while MPI-MTE shows a minimum in the Congo basin and higher values in arid zones like Sahel and South Africa. These discrepancies could, on the one hand, be ascribed to the limits of the bottom-up approach in dealing with the low seasonality of the fraction of absorbed radiation (FaPAR) in evergreen broadleaf forests, given the relevance of this predictor in the MPI-MTE estimates. A second reason for the discrepancy could be due to the CO₂ emissions from land use change that is particular relevant in some tropical areas but are not accounted in the MPI-MTE estimates. On the other hand, the fine-scale estimates of the inversion are largely determined by the a-priori weighting pattern, which has been chosen proportional to time-mean NPP (from the LPJ model) as a vegetation proxy (Rödenbeck et al., 2003). As the atmospheric data can only constrain larger-scale patterns comparable to the distances between the stations, this means that IAV will be locally higher where mean NPP is high, and vice versa.

As far as the Northern Hemisphere is concerned, a good correspondence is observed in western Eurasia, while some discrepancies are observed in other zones; for example MPI-MTE shows a large IAV in India, probably driven by the changes in FaPAR related to agricultural intensification, which is not emerging from the inversion product that has little observational constraint in this area. To summarize, the spatial pattern of IAV in the two products better agrees in the Northern Hemisphere for temperate and cold temperate zones, whereas for the southern Hemisphere, and in particular for the humid evergreen forests, they show a poor match. In general it has to be considered that both the MPI-MTE product and the Jena ~~inversion-Inversion~~ are driven by data from surface networks that are very ~~sparse-limited~~ in the Tropics and Southern Hemisphere and, therefore, these observation-driven estimates are under-constrained in those areas. These results highlight that for achieving more robust and consistent estimates of the terrestrial carbon fluxes it is of key importance to increase the availability of atmospheric and ecosystem flux observations in the Tropical region, either establishing new sites where the network is sparse or improving the sharing of data where the monitoring stations are available but not connected to global networks (e.g. flux stations in Amazonia).

The results presented in the maps of Figure 1 are summarized in the climate space in Figure 2. ~~The left panels show that peak values of IAV are located in different climate regions for the two gridded products (temperate humid for MPI-MTE, and tropical humid for Jena Inversion). In terms of absolute IAV, MPI-MTE shows the highest IAV at high temperature and intermediate precipitation levels, whereas Jena Inversion has its maximum in warm humid classes.~~

~~These results highlights that top-down and bottom-up estimates do not agree on the main sources of temporal variability in the terrestrial carbon budget and call for more investigation to pin down the reasons for these large discrepancies. Map pixels were classified according to mean annual temperature and precipitation, and the mean value of IAV_{NEE} and normalized IAV_{NEE} were calculated for each climate bin.~~

Given that the standard deviation of NEE increases with the primary productivity at the Fluxnet sites (Figure 3), ~~in Figure 2 (right column) we normalized IAV of both MPI-MTE and Jena inversion-Inversion by the average GPP of the specific climate bin from the MPI-MTE. Normalization using GPP (which that is always positive) offers a more robust metric of relative IAV if compared to normalization with NEE (-which fluctuates around zero) that spans across zero). Figure 2 reports in each climate bin either the mean IAV (left column) or (The ratio of the mean IAV and GPPs was plotted in the figure (right column), -since this metric is less sensitive to outliers than the mean of ratios ratios is more sensible to outliers, besides and -the former gives more weight to points that bear more information with larger fluxes.~~ The normalized IAV shows a consistent pattern between the three different data products, with a clear decreasing trend at increasing temperature and precipitation (i.e. increasing productivity). Ultimately arid regions seems to have the higher relative variation in land carbon fluxes, - which means that arid ecosystems show a higher variability in both data products, in accordance with previous findings (Ahlstrom et al., 2015). Interestingly the two gridded products show slightly different climatic location for the peak in relative IAV, with MPI-MTE pointing to warm arid regions whereas Jena Inversion points to cold arid systems.

~~In terms of absolute IAV, MPI-MTE shows the highest IAV at high temperature and intermediate precipitation levels, whereas Jena Inversion has its maximum in warm humid classes.~~

The dependency of IAV_{NEE} on GPP and on NEE_{CUP} is reported in Figure 3 for the three datasets. Both for Fluxnet and the Jena Inversion, IAV is positively related to increasing with either GPP or NEE_{CUP} . On the contrary, the IAV_{NEE} in the MPI-MTE dataset peaks at intermediate values of GPP and NEE_{CUP} , even if this trend is not evident in the Fluxnet data from which the MPI-MTE product is derived. ~~We think that this is due to the prominent role that FaPAR has in the MTE approach. Canopy greenness is particularly stable in the tropical humid forests (that are the most productive one) generating this unusual pattern of low relative IAV.~~ As stressed previously, ~~MPI-MTE this latter product~~ seems to underestimate the temporal variability of evergreen tropical forests both in South America and Africa, where the highest values of GPP and NEE_{CUP} are observed and where on the contrary the inversion shows high values of IAV. ~~We think that this mismatch is due to the prominent role that FaPAR has in the MTE approach. In fact, canopy greenness is particularly stable in the tropical humid forests, generating this unusual pattern of low relative IAV in regions of high productivity. These contrasting results for key regions like the Amazon and the Congo basin confirm the large uncertainty of the IAV estimates in areas with limited observational constraints. In these regions, climate sensitivities derived from estimates of the inter-annual variability of the terrestrial carbon budget have therefore to be carefully interpreted (Fang et al 2017).~~

The importance of the spatial scale of analysis on the IAV_{NEE} has been explored for both Fluxnet sites and the global products (i.e. MPI-MTE and Jena Inversion) (Figure 4). ~~Figure 4 shows the dependence of IAV_{NEE} on the spatial resolution of the analysis for Fluxnet sites and both global products (i.e. MPI-MTE and Jena Inversion) to verify if and to which extent the spatial scale is responsible for the differences observed between them.~~ The two global products show a good agreement at the native Inversion resolution ($5^\circ \times 3.75^\circ$) and at global level, when only one global value is retrieved by, spatially averaging all the pixels of the original maps. For the MPI-MTE product, the observed IAV is decreasing regularly at decreasing map resolution. On the contrary, the Jena Inversion shows a rapid descent followed by a stabilisation, probably

Formatted: Font color: Auto

Formatted: Font color: Auto

Comment [AC2]: 1. Fang, Y. et al. Global land carbon sink response to temperature and precipitation varies with ENSO phase. *Environ. Res. Lett.* **12**, 64007 (2017).

250 [due to a larger spatial coherence of the inversion signal compared to the MTE product. Fluxnet sites and their aggregation at](#)
[increasing distance also show a decreasing IAV with higher values compared to the global products. The slope of the lines in](#)
[Figure 4 reveals the degree of spatial compensation between anomalies \(steeper slopes are generated by stronger](#)
[compensation and therefore lower spatial coherence\), which leads to a decrease of \$IAV_{NEE}\$ at the increase of the spatial](#)
255 [extent of the observations. Among the three products MPI-MTE shows the more gentle slope and therefore the larger spatial](#)
[coherence of the anomalies. This is possibly due to the missing representation of land disturbances in the MTE methodology,](#)
[which may ultimately lead to an overestimation of the spatial coherence in the land \$CO_2\$ flux anomalies.](#)

The fractions of IAV_{NEE} generated either by temporal trends or by annual [anomalies-residuals](#) are summarized in Fig. 5 for the two global gridded products. For MPI-MTE, more than 80% of the IAV is explained by [anomalies-residuals](#) at all latitudes. Only in limited zones like Congo and Western Amazonia, MPI-MTE shows a relative minimum in the importance of [residualsanomalies](#), but this global product might underestimate the total variability in these zones (see Fig. 1b).
260 [Anomalies-Residuals](#) explain the largest share (between 62 and 90%, average 77%) of the temporal variability also in the Jena Inversion, with a higher relevance of trends in the southern hemisphere. The inversion product shows several hotspots of trend-driven variability, like [South Africa, South America](#) and northern Eurasia that is indeed reported as an area [of](#) increasing productivity in the last decades. In the interpretation of these results it is important to consider that MPI-MTE is generated by the statistical upscaling of Fluxnet data, using climate and FaPAR as predictors. This methodology relies on the assumption of a constant ecosystem response to climate drivers and for this reason the product cannot reproduce the influence of [some](#) environmental factors (e.g. increasing CO_2 concentration or nitrogen deposition) that [may](#) alter these responses [but-and that](#) are not reflected in input variables like [climate or](#) FaPAR. On the contrary, inversion products do not make any assumption on the climate dependence of ecosystem functioning, but include also emission from land management and land use change that may hide or emphasize the NEE trends. In summary, it is important to notice that, despite the
265 important climate trends, in the last 30 years the temporal variability of the land carbon balance has been driven by annual [anomaliesresiduals](#), confirming the dominant role of climate variability on the terrestrial C budget (Le Quéré et al., 2014).

For the two gridded products the analysis of IAV (either in terms of absolute IAV_{NEE} or normalized with NEE_{CUP}) was disaggregated by plant functional type (Figure 6). The analysis in terms of absolute IAV_{NEE} shows that savannas and woody savannas (WSAV-SAV) are the PFTs characterized by the larger IAV and variability within the PFT. This was found both for the MPI-MTE and the Jena Inversion product and confirms the results of a recent study (Ahlstrom et al., 2015) in which semi-arid ecosystems were found to account for the largest fraction (39%) of the global IAV in net biome productivity. This variability was found to be significantly related to the length of the growing season (Ma et al., 2007) [and is driven by the uncertainty in water supply in arid systems](#). In terms of normalized IAV the two gridded products show different behaviours,
270 CSH-OSH being the most variable PFT for MPI-MTE while the inversion data report a higher variability for EBF and WSAV-SAV. As observed at pixel scale in Figure 1, even at PFT level the results obtained from Fluxnet sites show a higher variability than the gridded products. In general at Fluxnet sites IAV is proportional to ecosystem productivity (Fig 4) with the maximum values observed in EBF, DBF-MF and CRO-GRA and the minimum in WET. The large value of IAV observed in GRA-CRO is presumably also affected by the potential large impact of management in these ecosystems that can either reduce (e.g. by irrigation) or increase the climate-induced variability (e.g. by changing crops or fertilization schemes, etc.). [In general the disaggregation of \$IAV_{NEE}\$ by PFTs shows rather similar results between the two gridded products, both in terms of magnitude and distribution. The largest difference is observed in the evergreen broadleaf forests whose absolute and relative variability is much larger in the inversion, possibly as a result of the intensive disturbances that have occurred in these ecosystems over the last decades and that are not captured with the MTE methodology.](#)
275
280
285

Formatted: Subscript

290 **3.2 Climate dependence of IAV**

The climatic dependence of the spatial variability of IAV_{NEE} at global scale for the MPI-MTE product (Figure 7) shows a clear pattern with positive correlations in temperature-limited areas at northern latitudes, and negative temperature dependence in water-limited zones (Braswell et al., 1997). These observations agree with Reichstein et al. (2007), which report that GPP shifts from soil water content to air temperature dependency at around 52° N. These opposite temperature dependences will probably lead to future contrasting changes in IAV. In fact, under a global warming scenario, the northern latitudes will be characterized by a larger sink (Zhao and Running, 2010) but also by a larger temporal variability, while arid zones like the Mediterranean basin, the Middle East Australia and the Sub-Saharan Africa will probably experience a reduction in IAV linked to large-scale droughts and consequent reduction in primary productivity (Ciais et al., 2005). Concerning precipitation the MPI-MTE product show more complex spatial patterns with negative correlation in the humid tropics, temperate Europe and South-East USA and positive correlation elsewhere.

The climate dependencies of IAV are further separated between the variability due to trends and anomalies (Fig. 78, Fig. 2 right column). The two components of IAV_{NEE} mostly show an agreement in the sign of the climatic controls, meaning that the environmental drivers have the same effects on trends and anomalies and therefore on the long and short time scales. This is a relevant finding because it, and therefore supports the use of IAV to investigate long-term-medium term climatic responses. An exception to this pattern is represented by the correlation with precipitation retrieved from MPI-MTE, which shows an unclear latitudinal pattern. In general anomalies show a higher correlation than trends, probably due to the larger magnitude of the variance attributed to this component. In conclusion, the spatial patterns shown in the maps of Fig. 7 and the agreement between the two components of IAV reported in the barplots indicate that the temperature controls of IAV of NEE is in general the same as for the primary productivity (i.e. positive in colder biomes and negative in warmer regions), while the contrasting results observed for precipitation suggest that the role played by water availability on the spatial and temporal variability is unclear, probably because of the temporal correlation between precipitation and temperature anomalies, as shows by Jung et al. (2017). The analysis of the climate drivers of IAV was not performed for the Jena inversion because for this product local variation in IAV are heavily driven by the prior estimates of NPP and therefore results have limited sensitivity to the atmospheric constraints. In fact, the optimization algorithm of the inversion spatially allocates the fluxes proportionally to the prior; hence grid-cells with higher productivity will change more if compared to cells with lower prior value (i.e. IAV at fine scale is proportional to the prior).

315 **3.3 Physiological drivers of IAV**

An improvement in the mechanistic understanding of IAV_{NEE} can be achieved by partitioning the net flux in its two components: GPP and TER. Partitioned fluxes are available for Fluxnet sites and for derived products like MPI-MTE, while they cannot be derived from atmospheric inversions. For this latter product the fluxes during the Carbon Uptake Period (CUP; $NEE < 0$) and during the Carbon Release Period (CRP; $NEE > 0$) were used in this analysis as proxies of GPP and TER, respectively.

To investigate how good these proxies are, the ratios TER/GPP during CUP and GPP/TER during CRP were analysed at Fluxnet sites and for each pixel of the MPI-MTE product and averaged by PFT (Figure 8a). As far as the MPI-MTE product is concerned, TER ranges from 55 to 78% of GPP during the CUP while GPP is 56 to 80% of TER during the CRP, hence on average about two-thirds of the signal come from GPP (TER) in the CUP (CRP). These ratios show a certain variability among PFTs, with ENF having the larger imbalance between the two fluxes and the lowest ratio TER/GPP during CUP (due to the strong seasonality of GPP in this PFT), while the two fluxes are not so well partitioned for EBFs (ratio ~0.8) that are characterized by a long growing season with consistently large fluxes of GPP and TER. The other PFTs show an average ratio value of ~0.65 both in CUP and CRP. In summary, it can be inferred that NEE during CUP is dominated by the signal of GPP, while NEE during CRP is dominated by TER even though to a smaller extent, as it emerges from the

frequency distributions in Figure 8bc calculated from the MPI-MTE product. The distribution of the ratio TER/GPP during the CUP is in fact narrower and peaks at a value of 0.7, while a broader distribution is observed for the GPP/TER ratio during the CRP. As expected there is a larger spread in the composition of NEE during CRP across the World, and this is linked to the larger variability in the seasonality of GPP that may actually go to zero in the dormancy season, while TER is always positive.

~~The difference between the variance explained by the two flux components (difference of the determination coefficients of the two regressions, where statistically significant) was used to determine which component (GPP vs TER or NEE_{CUP} vs NEE_{CRP}) drives the inter-annual variation of NEE. In order to identify which of the gross fluxes controls the variability of the net land flux we assessed the fraction of variance (R^2) of NEE explained by linear regressions were fitted on the NEE time series of each pixel/site against GPP or TER (for MPI-MTE and Fluxnet) and CUP or CRP (for all products). The difference between the variance explained by the two flux components (difference of the determination coefficients of the two regressions, where statistically significant) was used to determine which component (GPP vs TER or NEE_{CUP} vs NEE_{CRP}) drives the inter-annual variation of NEE. The aim of figure 9 Results reported in figure 9 show the difference of the determination coefficients between the two regressions (NEE versus GPP or TER; NEE versus NEE_{CUP} or NEE_{CRP}) and are used to determine which component dominates the inter-annual variation of NEE. is to highlight the role of GPP and TER (for MPI-MTE and Fluxnet) and of their proxy NEE_{CUP} and NEE_{CRP} (for Jena Inversion) in building up IAV_{NEE}. The determination coefficients were calculated for each pixel (for the gridded products) or site (for Fluxnet) fitting linear regressions of IAV_{NEE} vs either GPP (TER), or NEE_{CUP} (NEE_{CRP}). The difference in determination coefficients of GPP and TER linear regressions (the same holds for NEE_{CUP} and NEE_{CRP}) was used as a measure of which driver affects more IAV_{NEE}. Blue zones in figure 9 are regions where IAV_{NEE} is driven by photosynthesis (GPP/ or CUP), driven zones being the difference $R_{GPP}^2 - R_{TER}^2$ (or $R_{CUP}^2 - R_{CRP}^2$) positive, while in the red zones IAV_{NEE} areis mainly controlled by respiration (TER/ or CRP) driven. Figure 9a shows that, in most of the land area, the IAV_{NEE} is driven by GPP both at Fluxnet sites and for the MPI-MTE product. The same data products show an even clearer dominance of NEE_{CUP} on the IAV (Fig. 9b). The Jena Inversion product shows that, although most of the globe is NEE_{CUP} driven, there are quite a few areas that are weakly CRP driven like eastern US, arid regions in Africa and the Amazon basin, probably because these areas are estimated to be CO₂ sources in this inversion and therefore NEE is dominated by NEE_{CRP} (data not shown). When latitudinal profiles are considered, all the products show that GPP and NEE_{CUP} dominate control the temporal variability of yearly NEE more than TER or NEE_{CRP} (le Maire et al., 2010). Results shown in the global maps of Figure 9 are represented in the climatic space in Figure 10. Map pixels were classified according to mean annual temperature and precipitation. For each climate bin the difference between the determination coefficients for NEE vs GPP and TER is reported. Across the whole climate space, IAV retrieved from the MPI-MTE product is mostly controlled by CUP and GPP, although the difference in R^2 in the case of GPP and TER is low. The Jena Inversion on the contrary show climate areas where IAV is CRP driven, especially in intermediate-high temperature classes. Similar results have been reported across several PFT by Yuan et al., (2009) and Ahlstrom et al. (2015) using Fluxnet site data and MTE products. A higher correlation of IAV with GPP rather than with TER in deciduous forests has been reported also by Barr et al. (2002) and Wu et al. (2012). These results suggest that ecosystem fluxes during the CUP, and in particular photosynthesis more than respiration, are consistently controlling the inter-annual variability of NEE at all the spatial scales for both "bottom-up" and "top-down" data products (Janssens et al., 2001; Luyssaert et al., 2007; le Maire et al., 2010; Urbanski et al., 2007; Wohlfahrt et al., 2008a; Wu et al., 2012; Yuan et al., 2009). These results highlight that temporal variations of photosynthesis and of ecosystem CO₂ exchange during the carbon uptake period are therefore key driving to interpret the short-term climate sensitivity of the global carbon cycle consistently across different regions and climates. The possibility to interpret these short-term responses as long-term potential impacts of climate change is therefore to be disputed, given the limited role that respiration appears to play in modulating the rapid reactions of the terrestrial biosphere to environmental drivers.~~

Formatted: Superscript

Formatted: Subscript

375

380

385

390

In order to place our analysis in a broader context, global annual values of the gridded products used in the present analysis have been finally compared with the estimates of the Global Carbon Project (Figure 11). At annual timescale Jena Inversion shows an excellent agreement with the GCP, and this is not surprising since GCP land fluxes are estimated as residual term from the atmospheric CO₂ budget and are therefore not completely independent from the Jena Inversion product. On the other hand, this analysis highlights how the MTE bottom-up approach is barely correlated with the top-down estimates, both in term of trend and of anomalies. These discrepancies may be partially explained by the missing representation of land disturbances (land use change, land management) in the MTE product.

In conclusion, this study assessed the temporal variability of the terrestrial C budget with three different datasets to diagnose common patterns and emerging features. Some discrepancies between data-product have emerged, in particular in the Tropics where a chronic deficiency of atmospheric and ecosystem observations is severely limiting the accuracy of large-scale assessments. On the other hand, several important global features have been identified and confirmed by the different products like: i) the dominant role played by photosynthesis in the short-term variability of the land carbon budget, ii) the high relative IAV in water limited eco systems and iii) the dependence of IAV on spatial scales and ecosystem productivity. Ultimately, the variability of the land fluxes observed in the recent decades proved to be extremely valuable to investigate the controlling mechanisms, the sensitivity and vulnerability of the terrestrial C balance to climate drivers.

395 Figure 11 reports the results of the comparison of the two global products used in the present analysis with the Global Carbon Project dataset. The right panel shows the time series of annual anomalies of the three products. Jena Inversion shows a good agreement with the GCP, and this is not surprising since GCP land fluxes are estimated as residual term from the atmospheric CO₂ budget and are therefore not completely independent from the Jena Inversion product. On the other hand, this analysis highlights the well-known limits of the MPI-MTE product in representing the IAV.

400 **4 Conclusions**

Patterns and controls of the inter-annual variability of C_{carbon} net ecosystem exchange have been investigated using three different datasets: ecosystem level data from the FLUXNET database, the MPI-MTE bottom-up statistical upscaling of surface fluxes, and a top-down product based on atmospheric concentration data (Jena CarboScope CO₂ inversion).

405 The global average of site-level IAV_{NEE} ($-130 \text{ gC m}^{-2} \text{ y}^{-1}$), computed as the standard deviation of annual NEE, was observed to be almost 6 times the values calculated from the two global products (15 and 20 $\text{gC m}^{-2} \text{ y}^{-1}$ for MPI-MTE and Jena Inversion, respectively). This difference is probably due to the large variability in the spatial scale of point level and gridded products, combined with the scale dependence of the IAV signal, as shown in Fig 4 for the gridded products.

410 All datasets exhibited smaller IAV at higher latitudes, whereas arid ecosystems showed the largest IAV in the global products. Temperature has the highest correlation with the spatial patterns of IAV, with a positive control at temperature-limited northern ecosystems and a negative control in water-limited zones. Further insights in the sources of IAV have been achieved by exploring the temporal variability of the two gross components: GPP and TER. NEE fluxes during the carbon uptake and carbon release period were used as proxies of GPP and TER, respectively, since the partitioned fluxes were not available for the Jena Inversion. In all three datasets, GPP and NEE_{CUP}, respectively, were shown to control consistently the inter-annual variability NEE across geographical and climate domains, highlighting the fundamental role of photosynthesis in driving the temporal fluctuation of the land sink.

415 **ACKNOWLEDGEMENTS**

This study was supported by the JRC project AgForCC nr.442. The MCD12C1 product was retrieved from the online Data Pool, courtesy of the NASA EOSDIS Land Processes Distributed Active Archive Center (LP DAAC), USGS/Earth Resources Observation and Science (EROS) Center, Sioux Falls, South Dakota. This work used eddy covariance data acquired and shared by the FLUXNET community, including these networks: AmeriFlux, AfriFlux, AsiaFlux, CarboAfrica, CarboEuropeIP, CarboItaly, CarboMont, ChinaFlux, Fluxnet-Canada, GreenGrass, ICOS, KoFlux, LBA, NECC, OzFlux-TERN, TCOS-Siberia, and USCCC. The FLUXNET eddy covariance data processing and harmonization was carried out by the ICOS Ecosystem Thematic Center, AmeriFlux Management Project and Fluxdata project of FLUXNET, with the support of CDIAC, and the OzFlux, ChinaFlux and AsiaFlux offices.

420 GPPC Precipitation data provided by the NOAA/OAR/ESRL PSD, Boulder, Colorado, USA, from their Web site at <http://www.esrl.noaa.gov/psd/>

425 **References**

Ahlstrom, A., Raupach, M. R., Schurgers, G., Smith, B., Arneeth, A., Jung, M., Reichstein, M., Canadell, J. G., Friedlingstein, P., Jain, a. K., Kato, E., Poulter, B., Sitch, S., Stocker, B. D., Viovy, N., Wang, Y. P., Wiltshire, A., Zaehle, S. and Zeng, N.: The dominant role of semi-arid ecosystems in the trend and variability of the land CO₂ sink, Science (80-), 348(6237), 895–899, doi:10.1126/science.aaa1668, 2015.

430 Baker, D. F., Law, R. M., Gurney, K. R., Rayner, P., Peylin, P., Denning, A. S., Bousquet, P., Bruhwiler, L., Chen, Y., Ciais, P., Fung, I. Y., Heimann, M. and Nin, E.: TransCom 3 inversion intercomparison: Impact of transport model errors on the interannual variability of regional CO₂ fluxes, 1988–2003, 20, 1988–2003, doi:10.1029/2004GB002439, 2006.

- Bakwin, P., Davis, K., Yi, C. and Wofsy, S.: Regional carbon dioxide fluxes from mixing ratio data, *Tellus B*, 56, 301–311 [online] Available from: <http://onlinelibrary.wiley.com/doi/10.1111/j.1600-0889.2004.00111.x/full> (Accessed 9 November 2012), 2004.
- 435 Baldocchi, D.: TURNER REVIEW No. 15. “Breathing” of the terrestrial biosphere: Lessons learned from a global network of carbon dioxide flux measurement systems, *Aust. J. Bot.*, 56(1), 1–26, doi:10.1071/BT07151, 2008.
- Baldocchi, D., Falge, E., Gu, L., Olson, R., Hollinger, D., Running, S., Anthoni, P., Bernhofer, C., Davis, K., Evans, R., Fuentes, J., Goldstein, A., Katul, G., Law, B., Lee, X., Malhi, Y., Meyers, T., Munger, W., Oechel, W., Paw, K. T., Pilegaard, K., Schmid, H. P., Valentini, R., Verma, S., Vesala, T., Wilson, K. and Wofsy, S.: FLUXNET: A New Tool to Study the Temporal and Spatial Variability of Ecosystem–Scale Carbon Dioxide, Water Vapor, and Energy Flux Densities, *Bull. Am. Meteorol. Soc.*, 82(11), 2415–2434, doi:10.1175/1520-0477(2001)082<2415:FANTTS>2.3.CO;2, 2001.
- 440 Bousquet, P., Peylin, P., Ciais, P., Le Quere, C., Friedlingstein, P. and Tans, P. P.: Regional Changes in Carbon Dioxide Fluxes of Land and Oceans Since 1980, *Science* (80-.), 290(5495), 1342–1346, doi:10.1126/science.290.5495.1342, 2000.
- 445 Braswell, B., Schimel, D., Linder, E. and Moore, B.: The response of global terrestrial ecosystems to interannual temperature variability, *Science* (80-.), 278, 870–872 [online] Available from: <http://www.sciencemag.org/content/278/5339/870.short> (Accessed 9 November 2012), 1997.
- Ciais, P., Reichstein, M., Viovy, N., Granier, a, Ogé, J., Allard, V., Aubinet, M., Buchmann, N., Bernhofer, C., Carrara, a, Chevallier, F., De Noblet, N., Friend, a D., Friedlingstein, P., Grünwald, T., Heinesch, B., Keronen, P., Knohl, a, Krinner, G., Loustau, D., Manca, G., Matteucci, G., Miglietta, F., Ourcival, J. M., Papale, D., Pilegaard, K., Rambal, S., Seufert, G., Soussana, J. F., Sanz, M. J., Schulze, E. D., Vesala, T. and Valentini, R.: Europe-wide reduction in primary productivity caused by the heat and drought in 2003., *Nature*, 437(7058), 529–533, doi:10.1038/nature03972, 2005.
- 450 Cox, P. M., Betts, R. a, Jones, C. D., Spall, S. a and Totterdell, I. J.: Acceleration of global warming due to carbon-cycle feedbacks in a coupled climate model., *Nature*, 408(6809), 184–187, doi:10.1038/35041539, 2000.
- 455 Desai, A. R., Moorcroft, P. R., Bolstad, P. V. and Davis, K. J.: Regional carbon fluxes from an observationally constrained dynamic ecosystem model: Impacts of disturbance, CO₂ fertilization, and heterogeneous land cover, *J. Geophys. Res. Biogeosciences*, 112(1), 1–21, doi:10.1029/2006JG000264, 2007.
- Desai, A. R., Noormets, A., Bolstad, P. V., Chen, J., Cook, B. D., Davis, K. J., Euskirchen, E. S., Gough, C., Martin, J. G., Ricciuto, D. M., Schmid, H. P., Tang, J. and Wang, W.: Influence of vegetation and seasonal forcing on carbon dioxide fluxes across the Upper Midwest, USA: Implications for regional scaling, *Agric. For. Meteorol.*, 148(2), 288–308, doi:10.1016/j.agrformet.2007.08.001, 2008.
- 460 Desai, A. R., Helliker, B. R., Moorcroft, P. R., Andrews, A. E. and Berry, J. a.: Climatic controls of interannual variability in regional carbon fluxes from top-down and bottom-up perspectives, *J. Geophys. Res.*, 115(G2), G02011, doi:10.1029/2009JG001122, 2010.
- 465 Friedl, M. a. and Brodley, C. E.: Decision tree classification of land cover from remotely sensed data, *Remote Sens. Environ.*, 61(3), 399–409, doi:10.1016/S0034-4257(97)00049-7, 1997.
- Friedlingstein, P., Houghton, R. a, Marland, G., Hackler, J. L., Boden, T. a, Conway, T. J. and Al, E.: Update on CO₂ emissions, *Nat. Geosci.*, 2010(2007), 6–7, doi:10.1038/ngeo1022, 2010.
- 470 Gurney, K. R., Law, R. M., Denning, A. S., Rayner, P. J., Baker, D., Bousquet, P. and Bruhwiler, L.: Towards robust regional estimates of CO₂ sources and sinks using atmospheric transport models, *Nature*, 415(February), 626–630, 2002.
- Heimann, M. and Reichstein, M.: Terrestrial ecosystem carbon dynamics and climate feedbacks., *Nature*, 451(7176), 289–292, doi:10.1038/nature06591, 2008.
- Janssens, I. A., Lankreijer, H., Matteucci, G., Kowalski, A. S., Buchmann, N., Epron, D., Pilegaard, K., Kutsch, W., Longdoz, B., Grünwald, T., Montagnani, L., Dore, S., Rebmann, C., Moors, E. J., Grelle, A., Rannik, Ü., Morgenstern, K., Oltchev, S., Clement, R., Guomundsson, J., Minerbi, S., Berbigier, P., Ibrom, A., Moncrieff, J., Aubinet, M., Bernhofer, C., Jensen, N. O., Vesala, T., Granier, A., Schulze, E. D., Lindroth, A., Dolman, A. J., Jarvis, P. G., Ceulemans, R. and Valentini, R.: Productivity overshadows temperature in determining soil and ecosystem respiration across European forests, *Glob. Chang. Biol.*, 7(3), 269–278, doi:10.1046/j.1365-2486.2001.00412.x, 2001.
- 475 Jung, M., Reichstein, M. and Bondeau, A.: Towards global empirical upscaling of FLUXNET eddy covariance observations: validation of a model tree ensemble approach using a biosphere model, *Biogeosciences*, 6, 2001–2013 [online] Available from: <http://www.biogeosciences.net/6/2001/2009/bg-6-2001-2009.pdf>, 2009.
- Jung, M., Reichstein, M., Margolis, H. a., Cescatti, A., Richardson, A. D., Arain, M. A., Arneeth, A., Bernhofer, C., Bonal, D., Chen, J., Gianelle, D., Gobron, N., Kiely, G., Kutsch, W., Lasslop, G., Law, B. E., Lindroth, A., Merbold, L., Montagnani, L., Moors, E. J., Papale, D., Sottocornola, M., Vaccari, F. and Williams, C.: Global patterns of land-atmosphere fluxes of carbon dioxide, latent heat, and sensible heat derived from eddy covariance, satellite, and meteorological observations, *J. Geophys. Res.*, 116, G00J07, doi:10.1029/2010JG001566, 2011.
- 485 Jung, M., Reichstein, M., Schwalm, C. R., Huntingford, C. and Sitch, S.: Compensatory water effects link yearly global land CO₂ sink changes to temperature, *Nature*, (In Press), 2017.
- Leuning, R., Raupach, M. R., Coppin, P. a., Cleugh, H. a., Isaac, P., Denmead, O. T., Dunin, F. X., Zegelin, S. and Hacker,

- 490 J.: Spatial and temporal variations in fluxes of energy, water vapour and carbon dioxide during OASIS 1994 and 1995, *Boundary-Layer Meteorol.*, 110(1), 3–38, doi:10.1023/A:1026028217081, 2004.
- Lombardozi, D., Bonan, G. B. and Nychka, D. W.: The emerging anthropogenic signal in land–atmosphere carbon-cycle coupling, *Nat. Clim. Chang.*, 4(9), 796–800, doi:10.1038/nclimate2323, 2014.
- 495 Luysaert, S., Janssens, I. a., Sulkava, M., Papale, D., Dolman, a. J., Reichstein, M., Hollmén, J., Martin, J. G., Suni, T., Vesala, T., Loustau, D., Law, B. E. and Moors, E. J.: Photosynthesis drives anomalies in net carbon-exchange of pine forests at different latitudes, *Glob. Chang. Biol.*, 13(10), 2110–2127, doi:10.1111/j.1365-2486.2007.01432.x, 2007.
- Ma, S., Baldocchi, D. D., Xu, L. and Hehn, T.: Inter-annual variability in carbon dioxide exchange of an oak/grass savanna and open grassland in California, *Agric. For. Meteorol.*, 147(3–4), 157–171, doi:10.1016/j.agrformet.2007.07.008, 2007.
- 500 Mahadevan, P., Wofsy, S. C., Matross, D. M., Xiao, X., Dunn, A. L., Lin, J. C., Gerbig, C., Munger, J. W., Chow, V. Y. and Gottlieb, E. W.: A satellite-based biosphere parameterization for net ecosystem CO₂ exchange: Vegetation Photosynthesis and Respiration Model (VPRM), *Global Biogeochem. Cycles*, 22(2), doi:10.1029/2006GB002735, 2008.
- le Maire, G., Delpierre, N., Jung, M., Ciais, P., Reichstein, M., Viovy, N., Granier, A., Ibrom, A., Kolari, P., Longdoz, B., Moors, E. J., Pilegaard, K., Rambal, S., Richardson, A. D. and Vesala, T.: Detecting the critical periods that underpin interannual fluctuations in the carbon balance of European forests, *J. Geophys. Res.*, 115, G00H03, doi:10.1029/2009JG001244, 2010.
- 505 Marcolla, B., Cescatti, A., Manca, G., Zorer, R., Cavagna, M., Fiora, A., Gianelle, D., Rodeghiero, M., Sottocornola, M. and Zampedri, R.: Climatic controls and ecosystem responses drive the inter-annual variability of the net ecosystem exchange of an alpine meadow, *Agric. For. Meteorol.*, 151(9), 1233–1243, doi:10.1016/j.agrformet.2011.04.015, 2011.
- Morgenstern, K., Andrew Black, T., Humphreys, E. R., Griffis, T. J., Drewitt, G. B., Cai, T., Nescic, Z., Spittlehouse, D. L. and Livingston, N. J.: Sensitivity and uncertainty of the carbon balance of a Pacific Northwest Douglas-fir forest during an El Niño/La Niña cycle, *Agric. For. Meteorol.*, 123(3–4), 201–219, doi:10.1016/j.agrformet.2003.12.003, 2004.
- 510 Pacala, S. W.: Consistent Land- and Atmosphere-Based U.S. Carbon Sink Estimates, *Science* (80-.), 292(5525), 2316–2320, doi:10.1126/science.1057320, 2001.
- Papale, D. and Valentini, R.: A new assessment of European forests carbon exchanges by eddy fluxes and artificial neural network spatialization, *Glob. Chang. Biol.*, 9(4), 525–535, doi:10.1046/j.1365-2486.2003.00609.x, 2003.
- 515 Papale, D., Black, T. A., Carvalhais, N., Cescatti, A., Chen, J., Jung, M., Kiely, G., Lasslop, G., Mahecha, M. D., Margolis, H., Merbold, L., Montagnani, L., Moors, E., Olesen, J. E., Reichstein, M., Tramontana, G., van Gorsel, E., Wohlfahrt, G. and Ráduly, B.: Effect of spatial sampling from European flux towers for estimating carbon and water fluxes with artificial neural networks, *J. Geophys. Res. Biogeosciences*, 120(10), 1941–1957, doi:10.1002/2015JG002997, 2015.
- 520 Polley, H. W., Frank, A. B., Sanabria, J. and Phillips, R. L.: Interannual variability in carbon dioxide fluxes and flux–climate relationships on grazed and ungrazed northern mixed-grass prairie, *Glob. Chang. Biol.*, 14(7), 1620–1632, doi:10.1111/j.1365-2486.2008.01599.x, 2008.
- Polley, H. W., Emmerich, W., Bradford, J. a., Sims, P. L., Johnson, D. a., Saliendra, N. Z., Svejcar, T., Angell, R., Frank, A. B., Phillips, R. L., Snyder, K. a. and Morgan, J. a.: Physiological and environmental regulation of interannual variability in CO₂ exchange on rangelands in the western United States, *Glob. Chang. Biol.*, 16(3), 990–1002, doi:10.1111/j.1365-2486.2009.01966.x, 2010.
- 525 Poulter, B., Frank, D., Ciais, P., Myneni, R. B., Andela, N., Bi, J., Broquet, G., Canadell, J. G., Chevallier, F., Liu, Y. Y., Running, S. W., Sitch, S. and van der Werf, G. R.: Contribution of semi-arid ecosystems to interannual variability of the global carbon cycle, *Nature*, 509(7502), 600–603, doi:10.1038/nature13376, 2014.
- 530 Le Quere, C., Raupach, M. R., Canadell, J. G., Marland, G., Bopp, L., Ciais, P., Conway, T. J., Doney, S. C., Feely, R. a., Foster, P., Friedlingstein, P., Gurney, K., Houghton, R. a., House, J. I., Huntingford, C., Levy, P. E., Lomas, M. R., Majkut, J., Metzl, N., Ometto, J. P., Peters, G. P., Prentice, I. C., Randerson, J. T., Running, S. W., Sarmiento, J. L., Schuster, U., Sitch, S., Takahashi, T., Viovy, N., Werf, V. Der, Guido, R. and Woodward, F. I.: Trends in the sources and sinks of carbon dioxide, (November), 1–6, doi:10.1038/ngeo689, 2009.
- 535 Le Quéré, C., Peters, G. P., Andres, R. J., Andrew, R. M., Boden, T. a., Ciais, P., Friedlingstein, P., Houghton, R. a., Marland, G., Moriarty, R., Sitch, S., Tans, P., Arneth, a., Arvanitis, a., Bakker, D. C. E., Bopp, L., Canadell, J. G., Chini, L. P., Doney, S. C., Harper, a., Harris, I., House, J. I., Jain, a. K., Jones, S. D., Kato, E., Keeling, R. F., Klein Goldewijk, K., Körtzinger, a., Koven, C., Lefèvre, N., Maignan, F., Omar, a., Ono, T., Park, G. H., Pfeil, B., Poulter, B., Raupach, M. R., Regnier, P., Rödenbeck, C., Saito, S., Schwinger, J., Segsneider, J., Stocker, B. D., Takahashi, T., Tilbrook, B., Van Heuven, S., Viovy, N., Wanninkhof, R., Wiltshire, a. and Zaehle, S.: Global carbon budget 2013, *Earth Syst. Sci. Data*, 6(1), 235–263, doi:10.5194/essd-6-235-2014, 2014.
- 540 Reichstein, M., Papale, D., Valentini, R., Aubinet, M., Bernhofer, C., Knohl, A., Laurila, T., Lindroth, A., Moors, E., Pilegaard, K. and Seufert, G.: Determinants of terrestrial ecosystem carbon balance inferred from European eddy covariance flux sites, *Geophys. Res. Lett.*, 34(1), L01402, doi:10.1029/2006GL027880, 2007.
- 545 Richardson, A. D., Hollinger, D. Y., Aber, J. D., Ollinger, S. V. and Braswell, B. H.: Environmental variation is directly responsible for short- but not long-term variation in forest-atmosphere carbon exchange, *Glob. Chang. Biol.*, 13(4), 788–803,

- doi:10.1111/j.1365-2486.2007.01330.x, 2007.
- 550 Rödenbeck, C., Houweling, S., Gloor, M. and Heimann, M.: CO₂ flux history 1982–2001 inferred from atmospheric data using a global inversion of atmospheric transport, *Atmos. Chem. Phys.*, 3(6), 1919–1964, doi:10.5194/acp-3-1919-2003, 2003.
- Schneider, U., Becker, A., Finger, P., Meyer-Christoffer, A., Ziese, M. and Rudolf, B.: GPCP's new land surface precipitation climatology based on quality-controlled in situ data and its role in quantifying the global water cycle, *Theor. Appl. Climatol.*, 115(1–2), 15–40, doi:10.1007/s00704-013-0860-x, 2014.
- 555 Schultz, M. G., Heil, A., Hoelzemann, J. J., Spessa, A., Thonicke, K., Goldammer, J. G., Held, A. C., Pereira, J. M. C. and van Het Bolscher, M.: Global wildland fire emissions from 1960 to 2000, *Global Biogeochem. Cycles*, 22(2), 1–17, doi:10.1029/2007GB003031, 2008.
- Shao, J., Zhou, X., Luo, Y., Li, B., Aurela, M., Billesbach, D., Blanken, P. D., Bracho, R., Chen, J., Fischer, M., Fu, Y., Gu, L., Han, S., He, Y., Kolb, T., Li, Y., Nagy, Z., Niu, S., Oechel, W. C., Pinter, K., Shi, P., Suyker, A., Torn, M., Varlagin, A., Wang, H., Yan, J., Yu, G. and Zhang, J.: Biotic and climatic controls on interannual variability in carbon fluxes across terrestrial ecosystems, *Agric. For. Meteorol.*, 205, 11–22, doi:10.1016/j.agrformet.2015.02.007, 2015.
- 560 Stoy, P. C., Richardson, a. D., Baldocchi, D. D., Katul, G. G., Stanovick, J., Mahecha, M. D., Reichstein, M., Detto, M., Law, B. E., Wohlfahrt, G., Arriga, N., Campos, J., McCaughey, J. H., Montagnani, L., Paw U, K. T., Sevanto, S. and Williams, M.: Biosphere-atmosphere exchange of CO₂ in relation to climate: a cross-biome analysis across multiple time scales, *Biogeosciences*, 6(10), 2297–2312, doi:10.5194/bg-6-2297-2009, 2009.
- 565 Urbanski, S., Barford, C., Wofsy, S., Kucharik, C., Pyle, E., Budney, J., McKain, K., Fitzjarrald, D., Czikowsky, M. and Munger, J. W.: Factors controlling CO₂ exchange on timescales from hourly to decadal at Harvard Forest, *J. Geophys. Res.*, 112(G2), G02020, doi:10.1029/2006JG000293, 2007.
- Valentini, R., Matteucci, G., Dolman, a J., Schulze, E. D., Rebmann, C., Moors, E. J., Granier, a, Gross, P., Jensen, N. O., Pilegaard, K., Lindroth, a, Grelle, a, Bernhofer, C., Grünwald, T., Aubinet, M., Ceulemans, R., Kowalski, a S., Vesala, T., Rannik, U., Berbigier, P., Loustau, D., Gudmundsson, J., Thorgeirsson, H., Ibrom, a, Morgenstern, K. and Clement, R.: Respiration as the main determinant of carbon balance in European forests., *Nature*, 404(6780), 861–865, doi:10.1038/35009084, 2000.
- 570 Van Der Werf, G. R., Randerson, J. T., Giglio, L., Collatz, G. J., Mu, M., Kasibhatla, P. S., Morton, D. C., Defries, R. S., Jin, Y. and Van Leeuwen, T. T.: Global fire emissions and the contribution of deforestation, savanna, forest, agricultural, and peat fires (1997–2009), *Atmos. Chem. Phys.*, 10(23), 11707–11735, doi:10.5194/acp-10-11707-2010, 2010.
- 575 Wohlfahrt, G., Hammerle, A., Haslwanter, A., Bahn, M., Tappeiner, U. and Cernusca, A.: Seasonal and inter-annual variability of the net ecosystem CO₂ exchange of a temperate mountain grassland: effects of climate and management., *J. Geophys. Res. Atmos. JGR*, 113(D8), doi:10.1029/2007jd009286, 2008a.
- 580 Wohlfahrt, G., Hammerle, A., Haslwanter, A., Bahn, M., Tappeiner, U. and Cernusca, A.: Seasonal and inter-annual variability of the net ecosystem CO₂ exchange of a temperate mountain grassland: Effects of weather and management, *J. Geophys. Res.*, 113(D8), D08110, doi:10.1029/2007JD009286, 2008b.
- Wu, J., van der Linden, L., Lasslop, G., Carvalhais, N., Pilegaard, K., Beier, C. and Ibrom, A.: Effects of climate variability and functional changes on the interannual variation of the carbon balance in a temperate deciduous forest, *Biogeosciences*, 9(1), 13–28, doi:10.5194/bg-9-13-2012, 2012.
- 585 Yuan, W., Luo, Y., Richardson, A. D., Oren, R., Luysaert, S., Janssens, I. a., Ceulemans, R., Zhou, X., Grunwald, T., Aubinet, M., Berhofer, C., Baldocchi, D. D., Chen, J., Dunn, A. L., Deforest, J. L., Dragoni, D., Goldstein, A. H., Moors, E., William Munger, J., Monson, R. K., Suyker, A. E., Starr, G., Scott, R. L., Tenhunen, J., Verma, S. B., Vesala, T. and Wofsy, S. C.: Latitudinal patterns of magnitude and interannual variability in net ecosystem exchange regulated by biological and environmental variables, *Glob. Chang. Biol.*, 15(12), 2905–2920, doi:10.1111/j.1365-2486.2009.01870.x, 2009.
- 590 Zhao, M. and Running, S. W.: Drought-induced reduction in global terrestrial net primary production from 2000 through 2009., *Science*, 329(5994), 940–3, doi:10.1126/science.1192666, 2010.

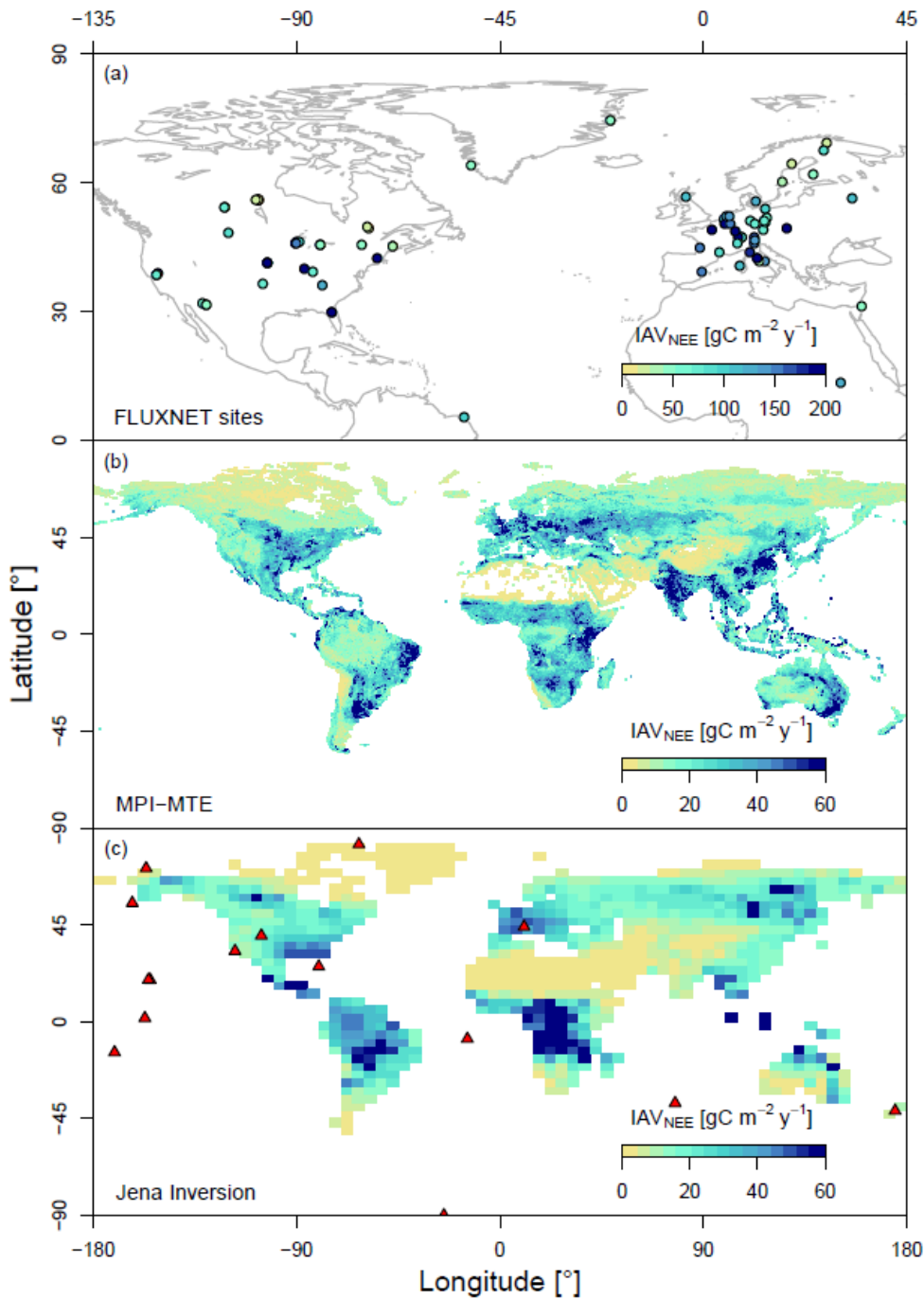
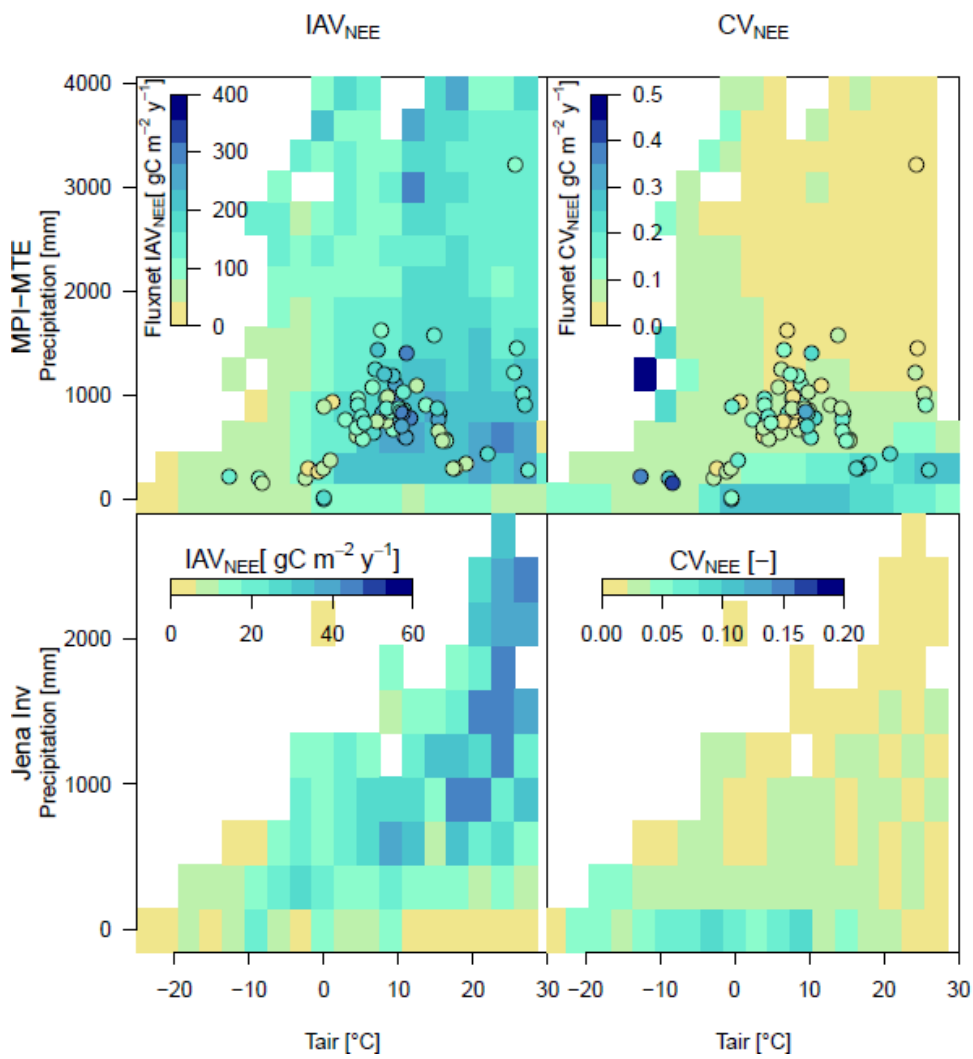


Figure 1: Spatial distribution of NEE standard deviation used as a measure of inter-annual variability (IAV_{NEE}). Results are reported for a) Fluxnet sites with at least 5 years of observations, b) for the MPI-MTE NEE product and c) Jena Inversion product s81_v3.6. red triangles represent the CO₂ concentration measurement sites.



600

Figure 2: IAV_{NEE} (left panels) and normalized IAV_{NEE} (CV_{NEE}, right panels) plotted in a Temperature-Precipitation space, for MPI-MTE (top panels) and Jena Inversion (bottom panels). Dots represent Fluxnet site values.

605

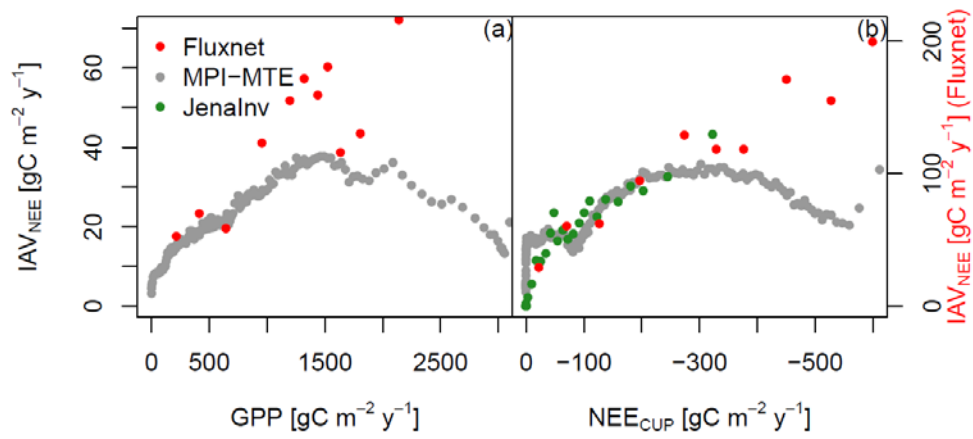
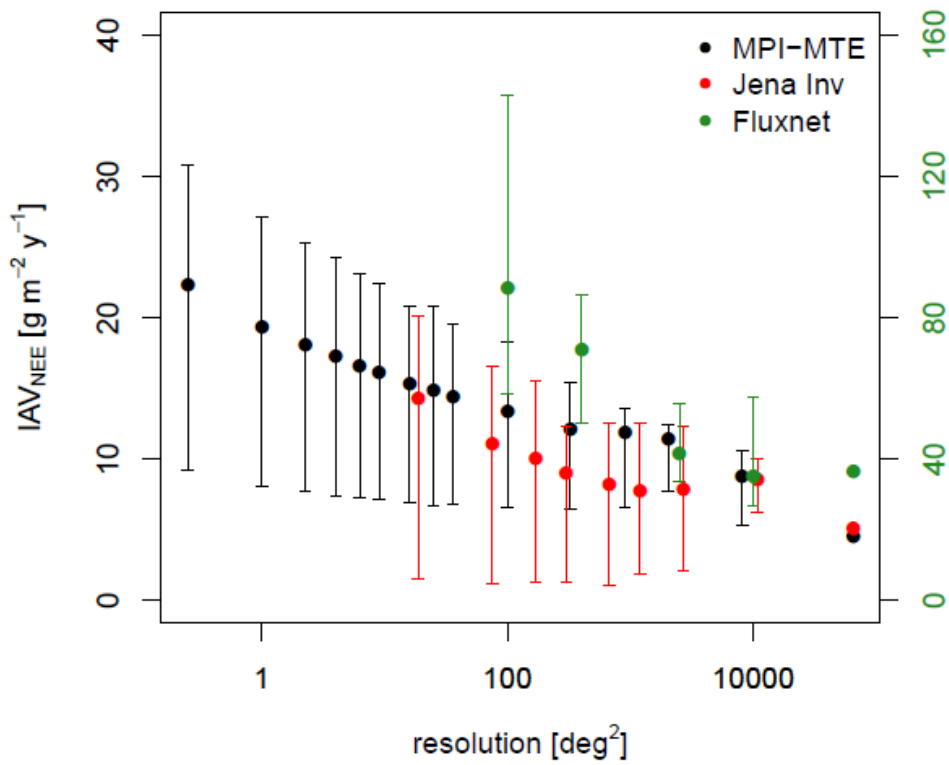


Figure 3: Dependency of standard deviation of NEE on GPP and NEE_{CUP}. Results are reported for Fluxnet sites (red dots, different y scale on the right), for the MPI-MTE NEE (black dots) and Jena Inversion product (green dots)



615 | Figure 4: Dependence of IAV_{NEE} on map resolution for [Fluxnet sites \(green dots\)](#), MPI-MTE (black dots) and Jena Inversion (red dots). Error bars represent the 25% and 75% quantiles of the IAV in the aggregated [sites/pixels](#).

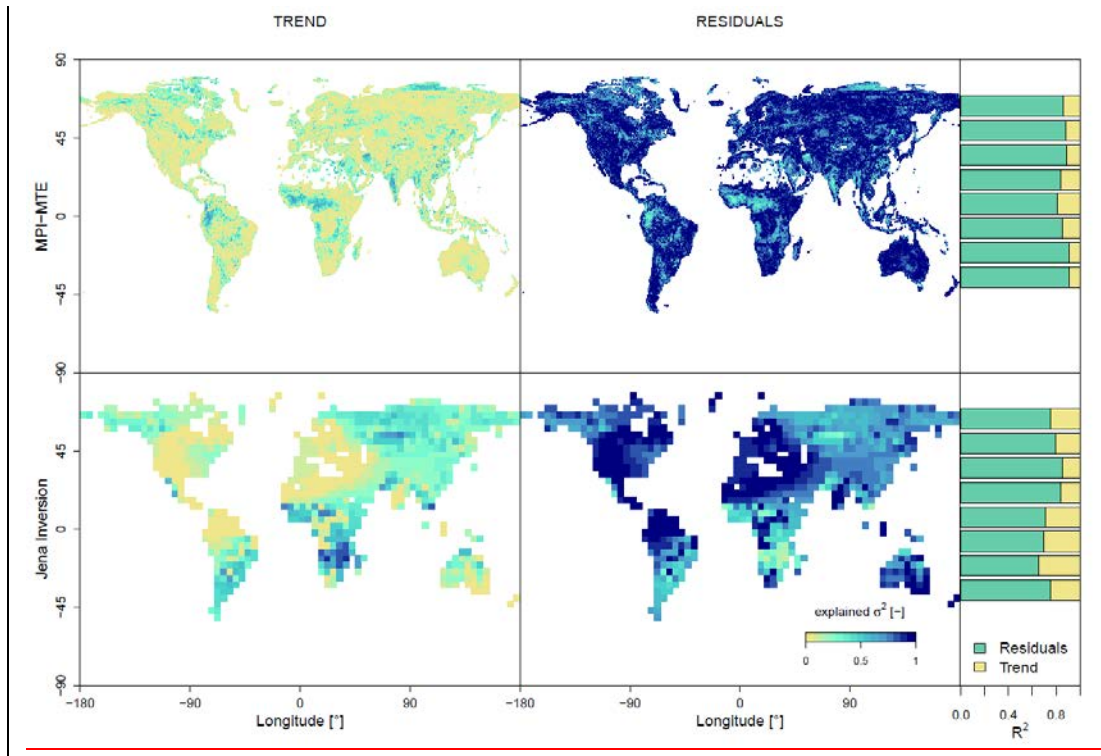
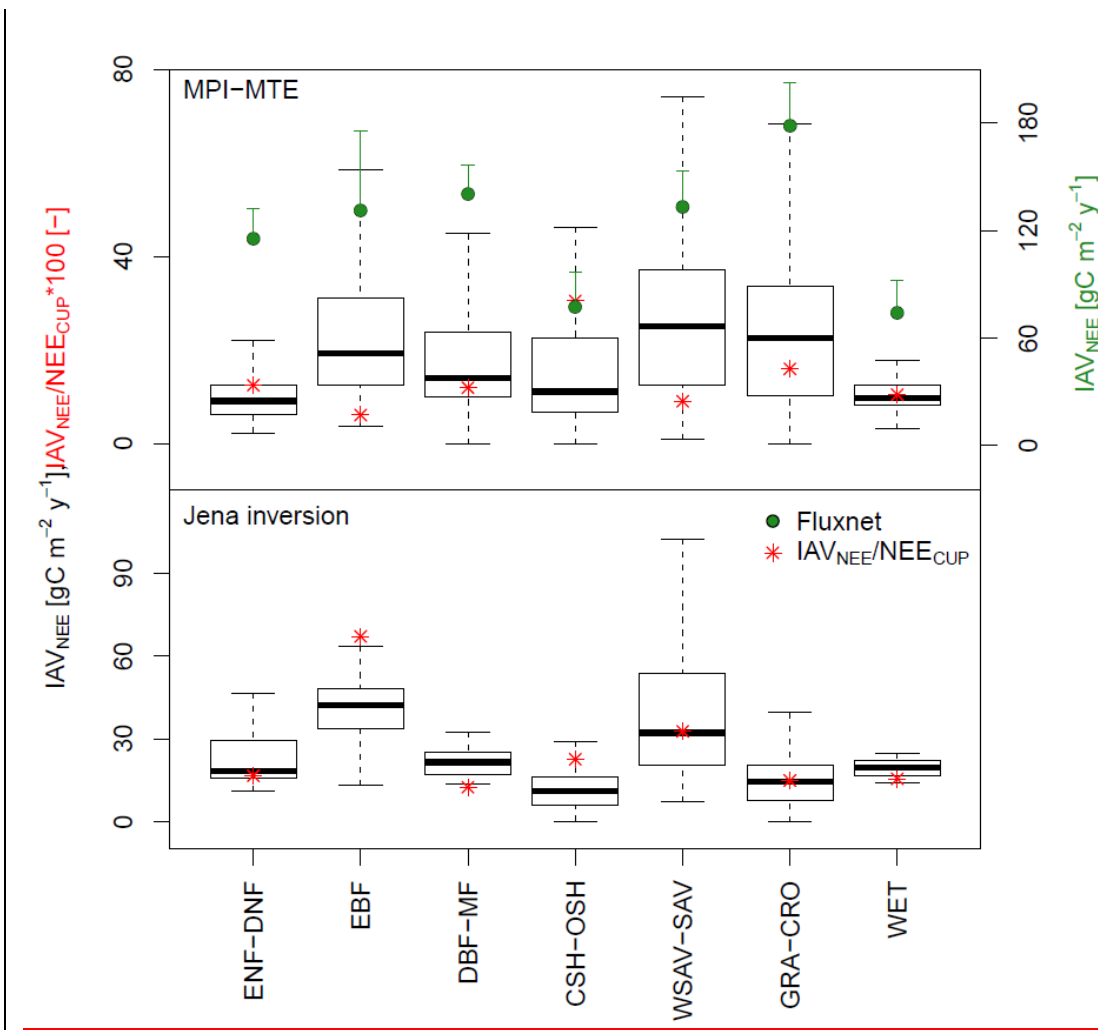


Figure 5: Maps of the fraction of NEE variance explained by temporal trends and anomalies for MPI-MTE NEE and Jena Inversion; latitudinal band (15°) averages of the fractions are reported in the bar plots.

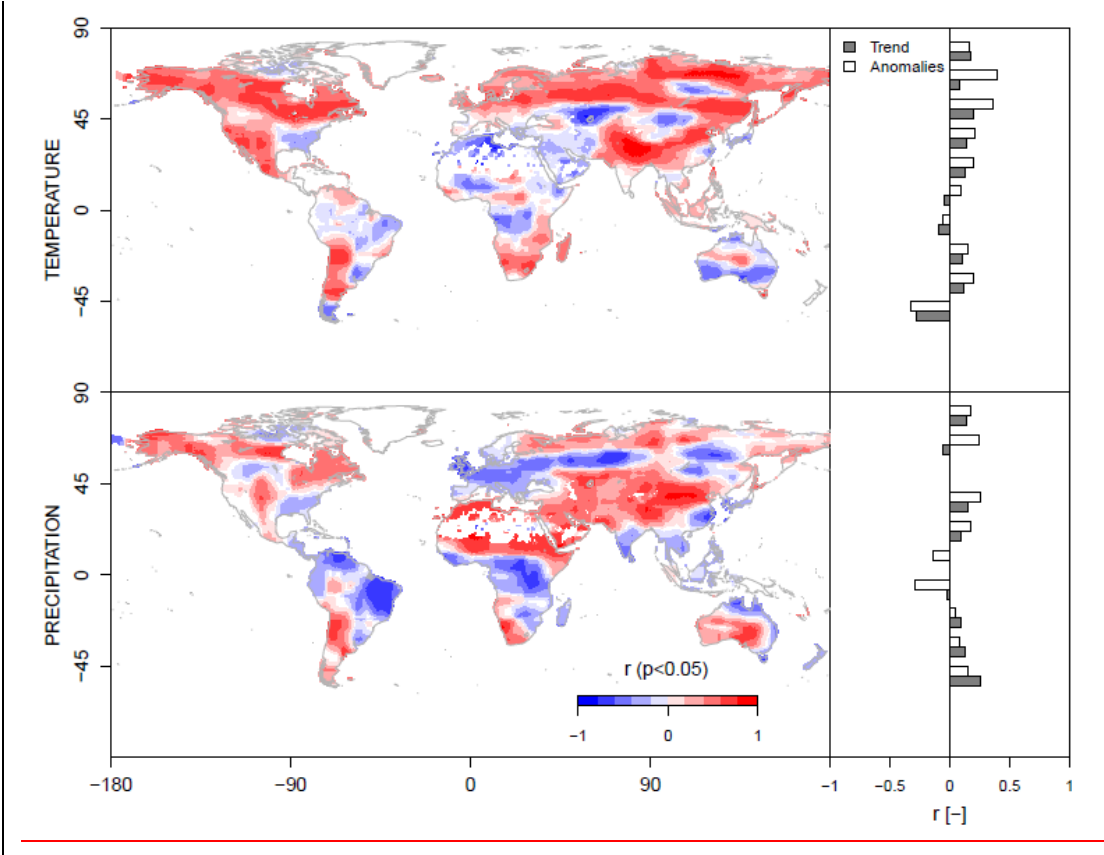
620



625

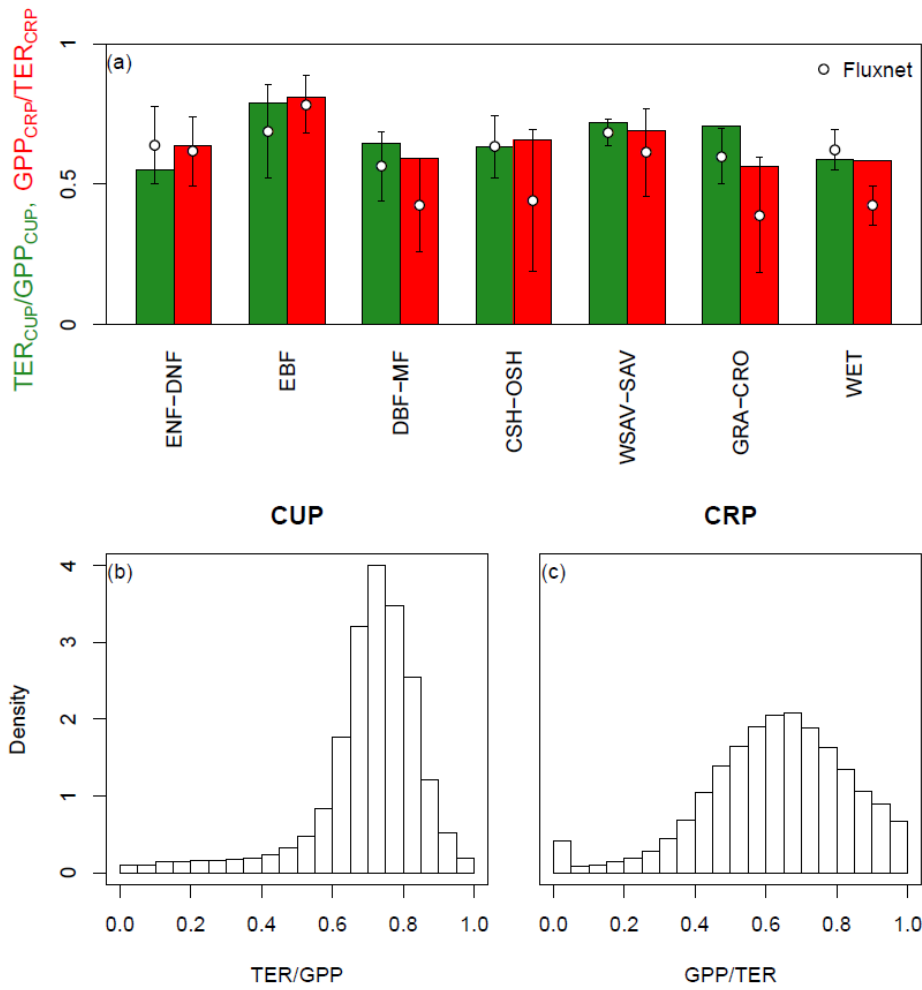
Figure 6: Boxplot of NEE standard deviation averaged in PFT classes for MPI-MTE NEE and Jena Inversion, green dots represent observations at Fluxnet sites (different y scale on the right) plotted with their standard error, PFT classes are grouped as follows: evergreen needleleaf forests and deciduous needleleaf forests (ENF-DNF), evergreen broadleaf forests (EBF), deciduous broadleaf forests and mixed forests (DBF-MF), closed and open shrublands (CSH-OSH), woody savannahs and savannahs (WSAV-SAV), grasslands and croplands (GRA-CRO) and wetlands (WET).

630



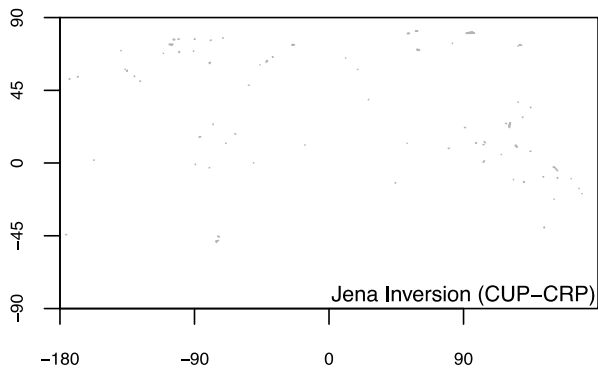
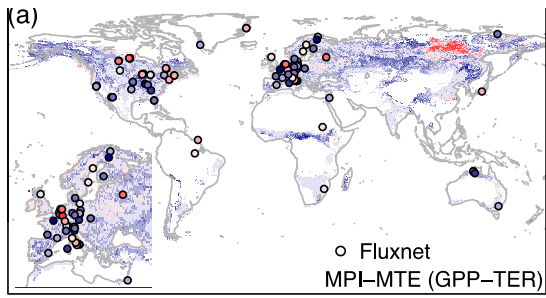
635 **Figure 7: Climatic drivers of the spatial variability of NEE standard deviation. The left panels show maps of the spatial correlation coefficients (within moving spatial windows of 15°x11.5°) of interannual NEE amplitude versus time-mean temperature and precipitation for the bottom up product MPI-MTE. Pixels with non-significant correlation are left white. The barplots on the right show latitudinal averages of the correlation coefficients of NEE trend and anomalies versus temperature and precipitation.**

640



645

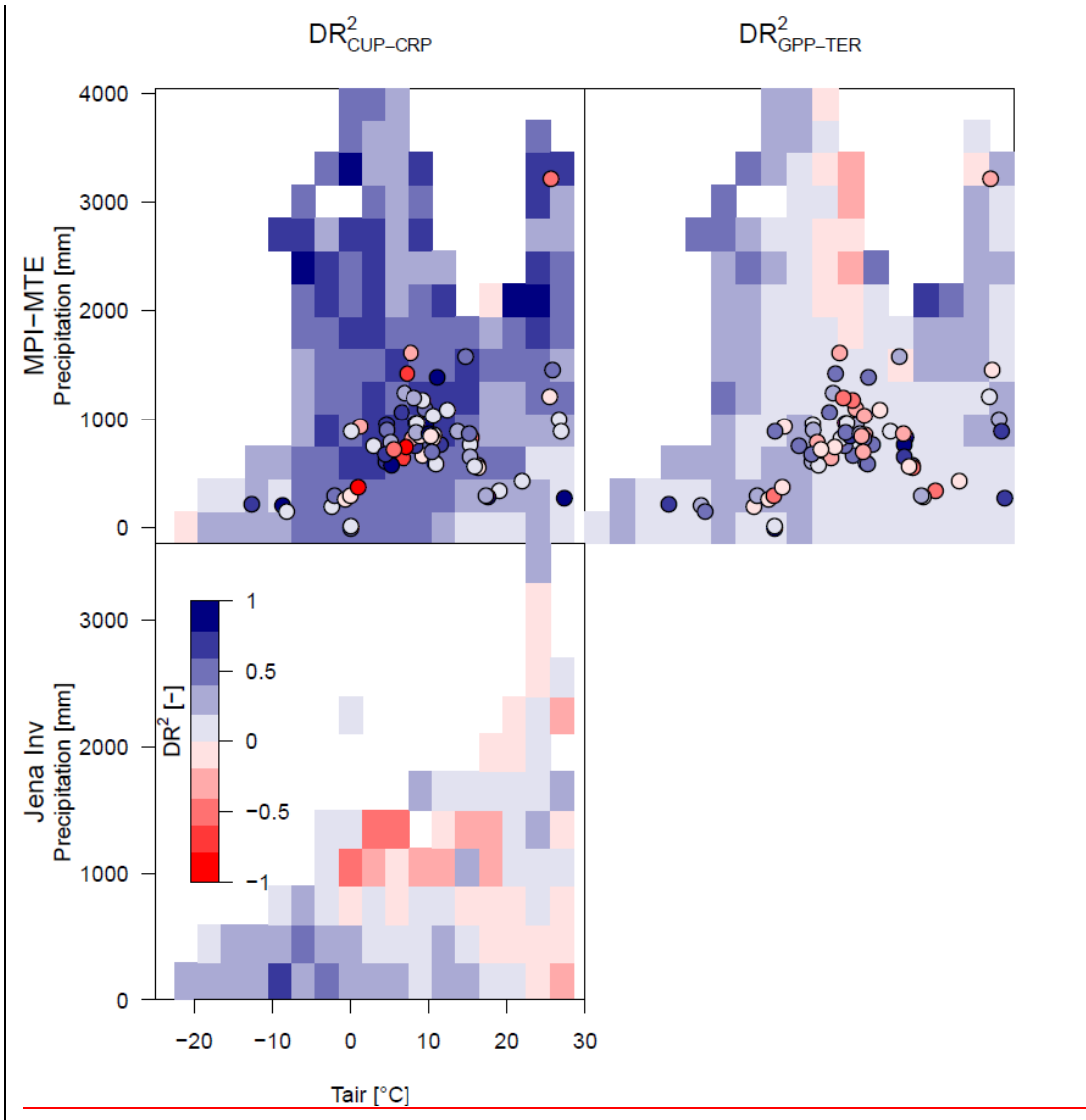
Figure 8: Bar plot of the ratio TER/GPP for the Carbon Uptake Period (CUP, green bars) and of the ratio GPP/TER during the Carbon Release Period (CRP, red bars), these values were calculated for the MPI-MTE product, dots refer to Fluxnet sites. Averages of yearly values are represented together with their standard deviation. The global frequency distributions of the ratios obtained from the MPI-MTE product are reported in the histograms at the bottom.



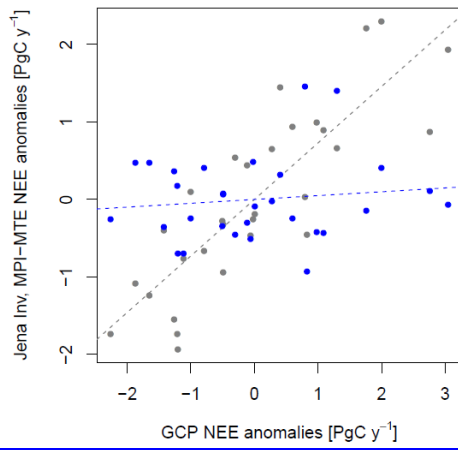
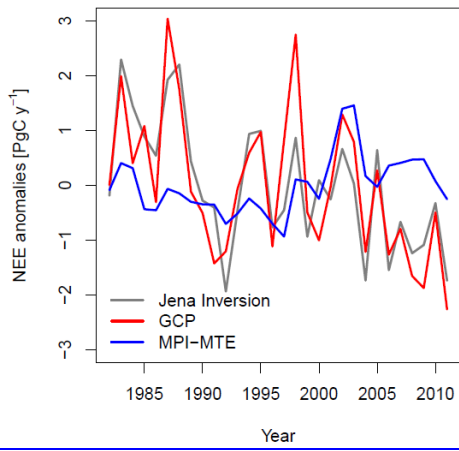
650

Figure 9: Control on IAV by GPP-TER and Carbon Uptake Period (CUP) - Carbon Release Period (CRP), expressed as the difference of the determination coefficients for Fluxnet sites with at least 5 years of observations (dots), MPI-MTE NEE and Jena Inversion. Latitudinal averages are reported for latitudinal classes of 15 degrees. Inset maps show an enlarged plot of Europe.

655



660 Figure 10: Control on IAV by GPP-TER and Carbon Uptake Period (CUP) - Carbon Release Period (CRP), expressed as the difference of the determination coefficients plotted in a Temperature Precipitation space. The two top panels refers to MPI-MTE while the bottom panel to Jena Inversion, dots refer to Fluxnet sites.



665

Figure 11: Comparison of the annual NEE anomalies between Jena Inversion, MPI-MTE and the Global Carbon Project data. Time series of annual anomalies are reported in the left panel while regressions of MPI-MTE and Jena Inversion values are reported in the right panel versus annual anomalies of the Global Carbon Project Data